APCTP-Pre2014-004

Non-linear matter bispectrum in general relativity

Sang Gyu Biern[a], Jinn-Ouk Gong[b,c] and Donghui Jeong[d]

[a] *Department of Physics, Seoul National University, Seoul 151-747, Korea*
[b] *Asia Pacific Center for Theoretical Physics, Pohang 790-784, Korea*
[c] *Department of Physics, Postech, Pohang 790-784, Korea*
[d] *Department of Physics and Astronomy, Johns Hopkins University, Baltimore, MD 21218, USA*

arXiv:1403.0438v1 [astro-ph.CO] 3 Mar 2014

Abstract

We show that the relativistic effects are negligibly small in the non-linear density and velocity bispectra. Although the non-linearities of Einstein equation introduce additional non-linear terms to the Newtonian fluid equations, the corrections to the bispectrum only show up on super-horizon scales. We show this with the next-to-leading order non-linear bispectrum for a pressureless fluid in a flat Friedmann-Robertson-Walker background, by calculating the density and velocity fields up to fourth order. We work in the comoving gauge, where the dynamics is identical to the Newtonian up to second order. We also discuss the leading order matter bispectrum in various gauges, and show yet another relativistic effect near horizon scales that the matter bispectrum strongly depends on the gauge choice.

1 Introduction

Recent advances in cosmology has been greatly spurred by precise cosmological observations. The accurate measurements of the temperature anisotropies and polarizations in the cosmic microwave background (CMB) by the Wilkinson Microwave Anisotropy Probe (WMAP) have opened the era of precision cosmology [1], and with the most recent PLANCK data we can constrain the cosmological parameters with less than $\mathcal{O}(1)$ percent error [2]. With the planned experiments such as PIXIE [3], PRISM [4], and LiteBIRD [5] to mention a few, it is guaranteed that we continue our success in the CMB observations and that we can constrain the cosmological parameters further and can obtain more information on the early universe as well.

Large scale structure (LSS) of the universe is yet another powerful cosmological probe, and its importance has ever been increasing with galaxy surveys such as SDSS [6], WiggleZ [7] and VIPERS [8]. The LSS observations can provide the measurement of geometrical distances, growth of structures, and shape of primordial correlation functions. These lower redshift information combined with the CMB data can break down the degeneracies among cosmological parameters that yields better constraints than CMB alone [2]. Furthermore, the full three-dimensional information with a huge redshift coverage available for the LSS observations naturally yields measurement of properties of dark energy, neutrino properties as well as physics of the early universe. A number of future observations such as HETDEX [10], MS-DESI [9], LSST [11] and Euclid [12] are proposed to observe LSS with improved accuracy in near future.

Provided that unprecedentedly accurate data will be soon available in both CMB and LSS, our theoretical endeavour should also meet the observational precision. This introduces, however, a number of interesting and important questions to be addressed, especially for LSS:

- Non-linearity: With increasing observational accuracy, we can probe the signal beyond the two-point correlation function in CMB and LSS. The higher-order correlation functions are the signature of non-linearities. Searching for the primordial non-Gaussianity [13] is a prime example. The current best constraint from PLANCK is consistent with that the primordial fluctuations follow the Gaussian statistics with the local non-linearity parameter $f_{\rm NL} = 2.7 \pm 5.8$ at 2σ confidence level. Non-linearity is more prominent in LSS: gravitational instability amplifies the density fluctuations to form non-linear structures such as galaxies and clusters of galaxies. As a result, the non-linearities deviates the matter power spectrum from the linear theory predictions [14, 15], and generates large higher-order correlation functions such as bispectrum and trispectrum. Accurate modeling of non-linearities is, therefore, the key requirement of exploiting the LSS data at the accuracy level similar to the CMB.

- Relevance of general relativity: Most studies on LSS in the past have been done in the context of the Newtonian gravity [16], which works fine in the small scale, sub-horizon limit. In order to achieve robust measurements of dark energy properties, for example from Baryon Acoustic Oscillations (See [17] for a recent review), planned future LSS surveys will probe larger and larger volume, and access the scales comparable to the horizon. Modeling the LSS observables on those large scales demands that we work in the fully general relativistic context. The first question that must be addressed is whether the purely relativistic effects are large enough to be detected or not. Furthermore, attempted modifications to general relativity (to explain the recent cosmic acceleration) mostly show up on such very large scales. Thus LSS is a perfect playground to test modified theories of gravity.

- Gauge: As we should resort to general relativity, at least in principle, to study LSS properly, it is crucial to clarify which 'gauge' we are using to interpret the data from LSS surveys. Different gauges are mathematically equivalent, but it does not mean that physical clarity is also equally shared. In particular, in the small scale limit the 'density contrasts' $\delta \equiv T^0{}_0/\overline{T}^0{}_0 - 1$ in almost all popular gauges are equivalent to the Newtonian density contrast [18], but equivalence does not hold on large enough scales close to the horizon. Of course, by properly choosing the gauge that we interpret the data, the gauge ambiguity on large scales disappears to yield the gauge invariant expression for the observable such as the galaxy power spectrum [19].

Bearing these in mind, we are encouraged to go beyond the two-point correlation function or power spectrum, and study the higher-order correlation functions arisen from the non-linearity in general relativity.

In this article, we study the next-to-leading order non-linearities in the matter bispectrum in the comoving gauge. The non-linear matter power spectrum in the same gauge was computed in [15]. In the comoving

gauge, the physical interpretation of the relativistic variables is transparent and the set of dynamical equations becomes particularly simple. Furthermore, the equations governing the dynamics of the density and velocity fields exactly coincide with the usual Newtonian hydrodynamic equations up to second order [20]. Therefore, the leading order matter bispectrum, which results from correlating one second order density contrast to two linear order ones, in the full relativistic calculation must be the same as that of the Newtonian calculation, and the purely relativistic contributions appear from the third order. To obtain the self-consistent next-to-leading order non-linearities, we calculate the density contrast to the fourth-order. We compute the one-loop matter density and velocity bispectra, and confirm that the purely relativistic corrections are subdominant on cosmologically relevant scales.

Going beyond the comoving gauge, we also calculate the leading order matter bispectrum from various other gauges to demonstrate the wild gauge dependence of the density and velocity bispectra. As in the case for the galaxy power spectrum, such a gauge dependence should go away when one calculate the 'observable' quantities in each gauge.

This article is organized as follows. In Section 2 we present the perturbation equations of a pressureless matter in the comoving gauge. In Section 3 we give the fourth order solutions of the perturbation equations in terms of kernels, and compute the matter bispectrum including one-loop corrections. In Section 4 we show the total bispectrum in particular configurations of interest. In Section 5 we show gauge dependence of the leading bispectrum in general relativity for large scale study. We conclude in Section 6.

2 Setup and equations

First we present the setup of the background around which we will introduce density contrast δ and the peculiar velocity $\boldsymbol{v}$. We consider a flat Friedmann-Robertson-Walker universe as a background. Furthermore, to simplify the analysis, we consider the Einstein-de Sitter universe, i.e. a flat Friedmann model dominated by a pressureless matter. This is a good enough approximation of our universe at high redshifts.

We find the Arnowitt-Deser-Misner formulation of 3+1 decomposition [21] particularly convenient for tracing the dynamical degrees of freedom in the system. The four-dimensional line element is given by

$$ds^2 = -N^2 dt^2 + \gamma_{ij}\left(N^i dt + dx^i\right)\left(N^j dt + dx^j\right) , \tag{1}$$

where N, N^i and γ_{ij} are, respectively, the lapse, shift and spatial metric. We use the Roman indices to indicate the spatial dimensions, which are raised and lowered by the spatial metric.

We only consider scalar perturbations, because the vector and tensor contributions may be negligibly small on scales where the relativistic effects are important. To fix the coordinate system, we choose the comoving gauge, which is defined by

$$T^0{}_i = 0\,. \tag{2}$$

This completely fixes the temporal gauge degree of freedom even at non-linear order [20]. The spatial gauge degree of freedom can be fixed by taking only a trace component of perturbation in the spatial metric,

$$\gamma_{ij} = a^2(1+2\varphi)\delta_{ij}\,. \tag{3}$$

The comoving gauge condition (2) gives rise to a particularly simple form of the energy-momentum tensor $T_{\mu\nu}$. We can write $T^\mu{}_\nu$ in the perfect fluid form

$$T^\mu{}_\nu = (\rho + p)u^\mu u_\nu + p\delta^\mu{}_\nu\,, \tag{4}$$

from which we can see that the comoving gauge condition demands $u_i = 0$. Then, for a pressureless matter, the energy and momentum densities and the spatial energy-momentum tensor which appear in the equations we are to solve are

$$\mathcal{E} \equiv N^2 T^{00} = \rho\,, \tag{5}$$

$$\mathcal{J}_i \equiv N T^0{}_i = 0\,, \tag{6}$$

$$\mathcal{S}_{ij} \equiv T_{ij} = 0\,. \tag{7}$$

This will lead to a great simplification of the equations.

Having the setup, we can now write the dynamical equations. The relevant equations are [22]

$$R^{(3)} + \frac{2}{3}K^2 - \overline{K}^i{}_j\overline{K}^j{}_i = 2\mathcal{E}\,, \tag{8}$$

$$\overline{K}^j{}_{i|j} - \frac{2}{3}K_{|i} = \mathcal{J}_i\,, \tag{9}$$

$$\mathcal{E}_{,0} - N^i\mathcal{E}_{,i} = NK\left(\mathcal{E} + \frac{\mathcal{S}}{3}\right) + N\overline{K}^i{}_j\overline{S}^j{}_i + \frac{1}{N}\left(N^2\mathcal{J}^i\right)_{|i}\,, \tag{10}$$

$$\mathcal{J}_{i,0} - N^j\mathcal{J}_{i,j} - N^j{}_{,i}\mathcal{J}_j = NK\mathcal{J}_i - \left(\mathcal{E}\delta^j{}_i + \mathcal{S}^j{}_i\right)N_{|j} - N\mathcal{S}^j{}_{i|j}\,, \tag{11}$$

$$K_{,0} - N^iK_{,i} = -N^{|i}{}_{|i} + N\left(R^{(3)} + K^2 + \frac{1}{2}\mathcal{S} - \frac{3}{2}\mathcal{E}\right)\,, \tag{12}$$

which are, respectively, the energy and momentum constraints, energy and momentum conservations, and the trace part of the evolution equation. Here, $R^{(3)}$ is the 3-curvature scalar constructed from γ_{ij}, K is the trace of the extrinsic curvature tensor $K_{ij} \equiv (N_{i|j} + N_{j|i} - \dot{\gamma}_{ij})/N$, an overbar denotes the traceless part, and a vertical bar denotes a covariant derivative with respect to γ_{ij}.

Now, applying our gauge conditions in the Einstein-de Sitter universe, from the momentum conservation we can see that $N_{,i} = 0$, i.e. the lapse function is homogeneous. Further, we can identify the perturbation variables as $\rho = \rho_0 + \delta\rho(t, \boldsymbol{x})$ and $K = 3H - \theta(t, \boldsymbol{x})$ with $\theta(t, \boldsymbol{x}) = \nabla \cdot \boldsymbol{v}(t, \boldsymbol{x})/a$, so that their equations in the comoving gauge exactly coincide with the Newtonian continuity and Euler equations respectively [20]. Then, from the energy and momentum constraint equations we can write respectively φ and N^i in terms of $\delta \equiv \delta\rho/\rho_0$ and $\boldsymbol{v}$. We arrive at the relativistic version of the continuity and Euler equations, which are up to fourth order:

$$\begin{aligned}\dot{\delta} + \frac{1}{a}\nabla\cdot\boldsymbol{v} =& -\frac{1}{a}\nabla\cdot(\delta\boldsymbol{v}) \\ &- \frac{1}{a}\left[-2\varphi_1\boldsymbol{v} + \nabla\left(\Delta^{-1}X_2\right)\right]\cdot(\nabla\delta) \\ &- \frac{1}{a}\left\{-2\varphi_2\boldsymbol{v} + \nabla\left(\Delta^{-1}X_3\right) - 2\varphi_1\left[-2\varphi_1\boldsymbol{v} + \nabla\left(\Delta^{-1}X_2\right)\right]\right\}\cdot(\nabla\delta)\,,\end{aligned} \tag{13}$$

$$\begin{aligned}&-\frac{1}{a}\nabla\cdot(\dot{\boldsymbol{v}} + H\boldsymbol{v}) - \frac{\rho_0}{2}\delta \\ =&\frac{1}{a^2}\nabla\cdot[(\boldsymbol{v}\cdot\nabla)\boldsymbol{v}] \\ &+ \frac{1}{a^2}\left(\Delta\left[(\boldsymbol{v}\cdot\nabla)\Delta^{-1}X_2\right] - (\boldsymbol{v}\cdot\nabla)X_2 - \frac{2}{3}X_2(\nabla\cdot\boldsymbol{v}) + \frac{2}{3}\varphi_1(\boldsymbol{v}\cdot\nabla)(\nabla\cdot\boldsymbol{v}) - 4\nabla\cdot\left\{\varphi_1\left[(\boldsymbol{v}\cdot\nabla)\boldsymbol{v} - \frac{1}{3}(\nabla\cdot\boldsymbol{v})\boldsymbol{v}\right]\right\}\right) \\ &+ \frac{1}{a^2}\left(\Delta\left[(\boldsymbol{v}\cdot\nabla)\Delta^{-1}X_3\right] - (\boldsymbol{v}\cdot\nabla)X_3 - \frac{2}{3}X_3(\nabla\cdot\boldsymbol{v}) + \frac{2}{3}\varphi_2(\boldsymbol{v}\cdot\nabla)(\nabla\cdot\boldsymbol{v}) - 4\nabla\cdot\left\{\varphi_2\left[(\boldsymbol{v}\cdot\nabla)\boldsymbol{v} - \frac{1}{3}(\nabla\cdot\boldsymbol{v})\boldsymbol{v}\right]\right\}\right. \\ &\quad - 4\nabla\cdot\left[\varphi_1\left\{\left[\nabla\left(\Delta^{-1}X_2\right)\right]\cdot\nabla - \frac{1}{3}X_2\right\}\boldsymbol{v} + \varphi_1\left\{(\boldsymbol{v}\cdot\nabla) - \frac{1}{3}(\nabla\cdot\boldsymbol{v})\right\}\left[\nabla(\Delta^{-1}X_2)\right]\right] \\ &\quad + \frac{2}{3}\varphi_1\left[\nabla(\nabla\cdot\boldsymbol{v})\cdot\nabla\left(\Delta^{-1}X_2\right) + 4(\boldsymbol{v}\cdot\nabla)X_2\right] + 12\nabla\cdot\left\{\varphi_1^2\left[(\boldsymbol{v}\cdot\nabla)\boldsymbol{v} - \frac{1}{3}(\nabla\cdot\boldsymbol{v})\boldsymbol{v}\right]\right\} - 4\varphi_1^2(\boldsymbol{v}\cdot\nabla)(\nabla\cdot\boldsymbol{v}) \\ &\quad \left. + 2(\nabla\varphi_1)\cdot(\nabla\varphi_1)\,\boldsymbol{v}\cdot\boldsymbol{v} + \frac{2}{3}(\nabla\varphi_1\cdot\boldsymbol{v})^2 + \nabla\cdot\left\{\left[\nabla\left(\Delta^{-1}X_2\right)\cdot\nabla\right]\nabla\left(\Delta^{-1}X_2\right) - X_2\nabla\left(\Delta^{-1}X_2\right)\right\} + \frac{2}{3}X_2^2\right)\,,\end{aligned} \tag{14}$$

where $\Delta \equiv \delta^{ij}\partial_i\partial_j$ and Δ^{-1} are spatial Laplacian and inverse Laplacian operators respectively, and

$$-\frac{\Delta}{a^2}\varphi_1 = \frac{\rho_0}{2}\delta - \frac{H}{a}\nabla\cdot\boldsymbol{v}\,, \tag{15}$$

$$-\frac{\Delta}{a^2}\varphi_2 = \frac{1}{4a^2}\left\{\nabla\cdot[(\boldsymbol{v}\cdot\nabla)\boldsymbol{v}] - (\boldsymbol{v}\cdot\nabla)(\nabla\cdot\boldsymbol{v}) - (\nabla\cdot\boldsymbol{v})^2\right\} - \frac{1}{2a^2}\left[3\,(\nabla\varphi_1)\cdot(\nabla\varphi_1) + 8\varphi_1\Delta\varphi_1\right]\,, \tag{16}$$

$$X_2 = 2\varphi_1\nabla\cdot\boldsymbol{v} - (\boldsymbol{v}\cdot\nabla)\varphi_1 + \frac{3}{2}\Delta^{-1}\nabla\cdot\left[\Delta\varphi_1\boldsymbol{v} + (\boldsymbol{v}\cdot\nabla)\,(\nabla\varphi_1)\right]\,, \tag{17}$$

$$\begin{aligned} X_3 =& 2\varphi_1 X_2 + 2\varphi_2(\nabla\cdot\boldsymbol{v}) - (\nabla\varphi_1)\cdot\left[\nabla\left(\Delta^{-1}X_2\right)\right] - (\boldsymbol{v}\cdot\nabla)\varphi_2 - 4\varphi_1^2(\nabla\cdot\boldsymbol{v}) + 4\varphi_1(\boldsymbol{v}\cdot\nabla)\varphi_1 \\ &+ \frac{3}{2}\Delta^{-1}\nabla\cdot\left[\Delta\varphi_1\nabla\left(\Delta^{-1}X_2\right) + \Delta\varphi_2\boldsymbol{v} + \nabla\left(\Delta^{-1}X_2\right)\cdot\nabla\,(\nabla\varphi_1) + (\boldsymbol{v}\cdot\nabla)\nabla\varphi_2\right] \\ &- \frac{3}{2}\Delta^{-1}\nabla\cdot\left\{(\nabla\varphi_1)\cdot(\nabla\varphi_1)\,\boldsymbol{v} + 3(\boldsymbol{v}\cdot\nabla)\varphi_1\nabla\varphi_1 + 4\varphi_1\left[(\boldsymbol{v}\cdot\nabla)\nabla\varphi_1 + \Delta\varphi_1\boldsymbol{v}\right]\right\}\,. \end{aligned} \tag{18}$$

Note that if $\varphi_1 = \varphi_2 = 0$, we recover the Newtonian continuity and Euler equations as can be read from (13) and (14), respectively. Thus, relativistic contributions are originated from φ_1 and φ_2.

3 One-loop bispectrum

3.1 Solutions

We can find the non-linear solutions of (13) and (14) perturbatively as follows. First the order linear solutions is the same as the standard ones for the linear perturbation theory,

$$\delta_1(\boldsymbol{k},t) = D(t)\delta_1(\boldsymbol{k},t_0)\,, \tag{19}$$

$$\theta_1(\boldsymbol{k},t) = -\,aHD(t)\delta_1(\boldsymbol{k},t_0)\,, \tag{20}$$

where $D(t)$ is the linear growth factor which is normalized to unity at the present time $t = t_0$, and $f \equiv d\log D/d\log a$ is the logarithmic derivative of the linear growth factor. Note that $D(t) = a(t)$ in the Einstein de-Sitter universe that we are considering here. With these linear solutions for density and velocity, we perturbatively expand the full non-linear solutions using momentum dependent symmetric kernels as

$$\delta(\boldsymbol{k},t) = \sum_{n=1}^{\infty}\delta_n = \sum_{n=1}^{\infty}D^n(t)\int\frac{d^3q_1\cdots d^3q_n}{(2\pi)^{3(n-1)}}\delta^{(3)}(\boldsymbol{k}-\boldsymbol{q}_{12\cdots n})F_n^{(s)}(\boldsymbol{q}_1,\cdots\boldsymbol{q}_n)\delta_1(\boldsymbol{q}_1)\cdots\delta_1(\boldsymbol{q}_n)\,, \tag{21}$$

$$\theta(\boldsymbol{k},t) = \sum_{n=1}^{\infty}\theta_n = -aH\sum_{n=1}^{\infty}D^n(t)\int\frac{d^3q_1\cdots d^3q_n}{(2\pi)^{3(n-1)}}\delta^{(3)}(\boldsymbol{k}-\boldsymbol{q}_{12\cdots n})G_n^{(s)}(\boldsymbol{q}_1,\cdots\boldsymbol{q}_n)\delta_1(\boldsymbol{q}_1)\cdots\delta_1(\boldsymbol{q}_n)\,, \tag{22}$$

where $F_1(\boldsymbol{k}) = G_1(\boldsymbol{k}) = 1$ and $\boldsymbol{q}_{12\cdots n} \equiv \sum_{i=1}^{n}\boldsymbol{q}_i$. Note that we only consider the fastest growing mode at each order in perturbations. With this ansatz, (13) and (14) become simply differential equations of F_n and G_n. Because the Newtonian hydrodynamical equations are closed at second order and the relativistic equations coincide with the Newtonian ones up to second order, the purely relativistic solutions appears from third order. Note that, in the comoving gauge, purely relativistic terms explicitly include the comoving horizon scale $k_H \equiv aH$.

The second order kernels are the same as standard perturbation theory [16], and the third order kernels are presented in (12) and (13) of [15]. For completeness, we present the equations and solutions for the fourth order kernels in Appendix A.

3.2 Tree bispectrum

The matter bispectrum is defined as

$$\langle\delta(\boldsymbol{k}_1,t)\delta(\boldsymbol{k}_2,t)\delta(\boldsymbol{k}_3,t)\rangle \equiv (2\pi)^3\delta^{(3)}(\boldsymbol{k}_{123})B(\boldsymbol{k}_1,\boldsymbol{k}_2,\boldsymbol{k}_3,t)\,, \tag{23}$$

and the velocity bispectrum is defined in the same way for $\theta(\boldsymbol{k},t)$. Assuming that the linear density perturbation δ_1 follows the Gaussian statistics, any higher order correlation functions beyond the linear power spectrum P_{11}, defined by

$$\langle\delta_1(\boldsymbol{k}_1,t)\delta_1(\boldsymbol{k}_2,t)\rangle \equiv (2\pi)^3\delta^{(3)}(\boldsymbol{k}_1+\boldsymbol{k}_2)P_{11}(k_1,t)\,, \tag{24}$$

can be written in terms of P_{11}. Note that from (20), we can see that the linear power spectrum of the velocity perturbation is simply P_{11} multiplied by $k_H^2 \equiv (aH)^2$. With Gaussian δ_1, the next-to-leading order bispectrum is given by

$$\begin{aligned}
&\langle\delta(\boldsymbol{k}_1)\delta(\boldsymbol{k}_2)\delta(\boldsymbol{k}_3)\rangle \\
=&\Big[\langle\delta_1(\boldsymbol{k}_1)\delta_1(\boldsymbol{k}_2)\delta_2(\boldsymbol{k}_3)\rangle + (2\text{ cyclic})\Big] \\
&+\langle\delta_2(\boldsymbol{k}_1)\delta_2(\boldsymbol{k}_2)\delta_2(\boldsymbol{k}_3)\rangle + \Big[\langle\delta_1(\boldsymbol{k}_1)\delta_1(\boldsymbol{k}_2)\delta_4(\boldsymbol{k}_3)\rangle + (2\text{ cyclic})\Big] + \Big[\langle\delta_1(\boldsymbol{k}_1)\delta_2(\boldsymbol{k}_2)\delta_3(\boldsymbol{k}_3)\rangle + (5\text{ cyclic})\Big] \\
\equiv&(2\pi)^3\delta^{(3)}(\boldsymbol{k}_{123})\Big\{B^{(0)}(\boldsymbol{k}_1,\boldsymbol{k}_2,\boldsymbol{k}_3) + \Big[B^{(1)}_{222}(\boldsymbol{k}_1,\boldsymbol{k}_2,\boldsymbol{k}_3) + B^{(1)}_{114}(\boldsymbol{k}_1,\boldsymbol{k}_2,\boldsymbol{k}_3) + B^{(1)}_{123}(\boldsymbol{k}_1,\boldsymbol{k}_2,\boldsymbol{k}_3)\Big]\Big\}\,,
\end{aligned} \tag{25}$$

where we have suppressed the time dependence notation. The leading bispectrum $B^{(0)}$ does not contain any internal momentum integration, and is thus usually dubbed as the "tree-level" bispectrum. Meanwhile, the leading corrections $B^{(1)}$ all contain one internal momentum integration and are frequently called as "one-loop" corrections. In the following, we present matter bispectrum only. The velocity bispectrum is obtained in essentially the same way by replacing the kernel G_i and supplying the additional factor $-k_H^3$.

We can straightforwardly compute the tree level bispectrum $B^{(0)}$. We first consider $\langle\delta_1(\boldsymbol{k}_1)\delta_1(\boldsymbol{k}_2)\delta_2(\boldsymbol{k}_3)\rangle$. This reads

$$\langle\delta_1(\boldsymbol{k}_1)\delta_1(\boldsymbol{k}_2)\delta_2(\boldsymbol{k}_3)\rangle = \int\frac{d^3q_1d^3q_2}{(2\pi)^3}\delta^{(3)}(\boldsymbol{k}_3-\boldsymbol{q}_{12})F_2^{(s)}(\boldsymbol{q}_1,\boldsymbol{q}_2)\Big\langle\delta_1(\boldsymbol{k}_1)\delta_1(\boldsymbol{k}_2)\Big[\delta_1(\boldsymbol{q}_1)\delta_1(\boldsymbol{q}_2)\Big]\Big\rangle\,. \tag{26}$$

Then, we can immediately find

$$\langle\delta_1(\boldsymbol{k}_1)\delta_1(\boldsymbol{k}_2)\delta_2(\boldsymbol{k}_3)\rangle = (2\pi)^3\delta^{(3)}(\boldsymbol{k}_{123})2F_2^{(s)}(-\boldsymbol{k}_1,-\boldsymbol{k}_2)P_{11}(k_1)P_{11}(k_2)\,, \tag{27}$$

and the tree bispectrum is thus

$$B^{(0)}(\boldsymbol{k}_1,\boldsymbol{k}_2,\boldsymbol{k}_3) = 2F_2^{(s)}(-\boldsymbol{k}_1,-\boldsymbol{k}_2)P_{11}(k_1)P_{11}(k_2) + (2\text{ cyclic})\,. \tag{28}$$

3.3 One-loop bispectrum

3.3.1 $B^{(1)}_{222}$

Next we consider the first one-loop correction term, $B^{(1)}_{222}(\boldsymbol{k}_1,\boldsymbol{k}_2,\boldsymbol{k}_3)$. From the full expression

$$\begin{aligned}
\langle\delta_2(\boldsymbol{k}_1)\delta_2(\boldsymbol{k}_2)\delta_2(\boldsymbol{k}_3)\rangle =& \int\frac{d^3q_1\cdots d^3q_2}{(2\pi)^{3\cdot3}}\delta^{(3)}(\boldsymbol{k}_1-\boldsymbol{q}_{12})\delta^{(3)}(\boldsymbol{k}_2-\boldsymbol{q}_{34})\delta^{(3)}(\boldsymbol{k}_3-\boldsymbol{q}_{56}) \\
&\times F_2^{(s)}(\boldsymbol{q}_1,\boldsymbol{q}_2)F_2^{(s)}(\boldsymbol{q}_3,\boldsymbol{q}_4)F_2^{(s)}(\boldsymbol{q}_5,\boldsymbol{q}_6)\Big\langle\Big[\delta_1(\boldsymbol{q}_1)\delta_1(\boldsymbol{q}_2)\Big]\Big[\delta_1(\boldsymbol{q}_3)\delta_1(\boldsymbol{q}_4)\Big]\Big[\delta_1(\boldsymbol{q}_5)\delta_1(\boldsymbol{q}_6)\Big]\Big\rangle\,,
\end{aligned} \tag{29}$$

we can find

$$\begin{aligned}
B^{(1)}_{222}(\boldsymbol{k}_1,\boldsymbol{k}_2,\boldsymbol{k}_3) =& 8\int\frac{d^3q}{(2\pi)^3}F_2^{(s)}(\boldsymbol{q},\boldsymbol{k}_1-\boldsymbol{q})F_2^{(s)}(-\boldsymbol{q},\boldsymbol{k}_2+\boldsymbol{q})F_2^{(s)}(-\boldsymbol{k}_1+\boldsymbol{q},-\boldsymbol{k}_2-\boldsymbol{q}) \\
&\times P_{11}(q)P_{11}(|\boldsymbol{k}_1-\boldsymbol{q}|)P_{11}(|\boldsymbol{k}_2+\boldsymbol{q}|)\,.
\end{aligned} \tag{30}$$

3.3.2 $B^{(1)}_{114}$

For the next term $B^{(1)}_{114}(\boldsymbol{k}_1,\boldsymbol{k}_2,\boldsymbol{k}_3)$, we can proceed in the same manner. Let us consider

$$\begin{aligned}
\langle\delta_1(\boldsymbol{k}_1)\delta_1(\boldsymbol{k}_2)\delta_4(\boldsymbol{k}_3)\rangle =& \int\frac{d^3q_1\cdots d^3q_4}{(2\pi)^{3\cdot3}}\delta^{(3)}(\boldsymbol{k}_3-\boldsymbol{q}_{1234}) \\
&\times F_4^{(s)}(\boldsymbol{q}_1,\boldsymbol{q}_2,\boldsymbol{q}_3,\boldsymbol{q}_4)\Big\langle\delta_1(\boldsymbol{k}_1)\delta_1(\boldsymbol{k}_2)\Big[\delta_1(\boldsymbol{q}_1)\delta_1(\boldsymbol{q}_2)\delta_1(\boldsymbol{q}_3)\delta_1(\boldsymbol{q}_4)\Big]\Big\rangle\,.
\end{aligned} \tag{31}$$

Then after straightforward calculations we find

$$B^{(1)}_{114}(\boldsymbol{k}_1,\boldsymbol{k}_2,\boldsymbol{k}_3) = 12\int\frac{d^3q}{(2\pi)^3}F_4^{(s)}(-\boldsymbol{k}_1,-\boldsymbol{k}_2,\boldsymbol{q},-\boldsymbol{q})P_{11}(k_1)P_{11}(k_2)P_{11}(q) + (2\text{ cyclic})\,. \tag{32}$$

3.3.3 $B^{(1)}_{123}$

Finally, we consider the last contribution $B^{(1)}_{123}(\boldsymbol{k}_1,\boldsymbol{k}_2,\boldsymbol{k}_3)$ with

$$\langle\delta_1(\boldsymbol{k}_1)\delta_2(\boldsymbol{k}_2)\delta_3(\boldsymbol{k}_3)\rangle = \int\frac{d^3q_1\cdots d^3q_5}{(2\pi)^{3\cdot3}}\delta^{(3)}(\boldsymbol{k}_2-\boldsymbol{q}_{12})\delta^{(3)}(\boldsymbol{k}_3-\boldsymbol{q}_{345}) \times F_2^{(s)}(\boldsymbol{q}_1,\boldsymbol{q}_2)F_3^{(s)}(\boldsymbol{q}_3,\boldsymbol{q}_4,\boldsymbol{q}_5)\Big\langle\delta_1(\boldsymbol{k}_1)\Big[\delta_1(\boldsymbol{q}_1)\delta_1(\boldsymbol{q}_2)\Big]\Big[\delta_1(\boldsymbol{q}_3)\delta_1(\boldsymbol{q}_4)\delta_1(\boldsymbol{q}_5)\Big]\Big\rangle\,. \tag{33}$$

There are two different ways of correlating the six δ_1's. Let us call them (a) and (b). First, (a) is that the two propagators from δ_2 vertex are connected to both δ_1 and δ_3 vertices, and the remaining two propagators within δ_3 are inter-connected and form a loop. And (b) is that the two propagators from δ_2 vertex are both connected to δ_3 vertex, and the remaining one propagator of δ_3 is connected to δ_1 vertex. That is, in terms of momentum shown in (33), (a) corresponds to the correlations that one of $\{\boldsymbol{q}_1,\boldsymbol{q}_2\}$ is correlated to $\boldsymbol{k}_1$, and the remaining one is correlated to $\{\boldsymbol{q}_3,\boldsymbol{q}_4,\boldsymbol{q}_5\}$. For (b), two of $\{\boldsymbol{q}_3,\boldsymbol{q}_4,\boldsymbol{q}_5\}$ are correlated to $\{\boldsymbol{q}_1,\boldsymbol{q}_2\}$, and the remaining one is correlated to $\boldsymbol{k}_1$. There are six non-zero contributions for each of (a) and (b), and we work out to find

$$B^{(1)}_{123}(\boldsymbol{k}_1,\boldsymbol{k}_2,\boldsymbol{k}_3) = B^{(1)}_{123a}(\boldsymbol{k}_1,\boldsymbol{k}_2,\boldsymbol{k}_3) + B^{(1)}_{123b}(\boldsymbol{k}_1,\boldsymbol{k}_2,\boldsymbol{k}_3)\,, \tag{34}$$

$$B^{(1)}_{123a}(\boldsymbol{k}_1,\boldsymbol{k}_2,\boldsymbol{k}_3) = 6F_2^{(s)}(-\boldsymbol{k}_1,-\boldsymbol{k}_3)\int\frac{d^3q}{(2\pi)^3}F_3^{(s)}(\boldsymbol{k}_3,\boldsymbol{q},-\boldsymbol{q})P_{11}(k_1)P_{11}(k_3)P_{11}(q) + (5\text{ cyclic})\,, \tag{35}$$

$$B^{(1)}_{123b}(\boldsymbol{k}_1,\boldsymbol{k}_2,\boldsymbol{k}_3) = 6\int\frac{d^3q}{(2\pi)^3}F_2^{(s)}(\boldsymbol{q},\boldsymbol{k}_2-\boldsymbol{q})F_3^{(s)}(-\boldsymbol{k}_1,-\boldsymbol{k}_2+\boldsymbol{q},-\boldsymbol{q})P_{11}(k_1)P_{11}(q)P_{11}(|\boldsymbol{k}_2-\boldsymbol{q}|) + (5\text{ cyclic})\,. \tag{36}$$

One can find the diagramatic representation of the one-loop bispectrum in [23].

4 Results

To highlight the general relativistic effect at one-loop level, we find it sufficient to show some special triangular configurations. We set the three momenta $\boldsymbol{k}_1$, $\boldsymbol{k}_2$ and $\boldsymbol{k}_3$ in such a way that $|\boldsymbol{k}_1|=|\boldsymbol{k}_2|=k$ and $|\boldsymbol{k}_3|=k/\alpha$, and vary α for different configurations of interest. For example, $\alpha=1/2$, $\alpha=1$ and $\alpha\gg1$ correspond to the folded, equilateral and squeezed configurations, respectively. We implement the integration in the one-loop calculation by setting $\boldsymbol{k}_1$, $\boldsymbol{k}_2$ and $\boldsymbol{k}_3$ on the xz plane with $\boldsymbol{k}_1$ being aligned along the z axis. To perform the integration over $\boldsymbol{q}$, we introduce the magnitude of $\boldsymbol{q}$ and the cosine between $\boldsymbol{q}$ and $\boldsymbol{k}_1$ as $q=rk$ and $\boldsymbol{k}_1\cdot\boldsymbol{q}=k^2r\mu$ with $0\le r\le\infty$ and $-1\le\mu\le1$. Then, each vector including the internal momentum $\boldsymbol{q}$ is given respectively by

$$\boldsymbol{k}_1 = (0,0,k)\,, \tag{37}$$

$$\boldsymbol{k}_2 = \left(\frac{\sqrt{4\alpha^2-1}}{2\alpha^2}k, 0, \frac{1-2\alpha^2}{2\alpha^2}k\right)\,, \tag{38}$$

$$\boldsymbol{k}_3 = -\boldsymbol{k}_1-\boldsymbol{k}_3\,, \tag{39}$$

$$\boldsymbol{q} = \left(kr\sqrt{1-\mu^2}\cos\phi, kr\sqrt{1-\mu^2}\sin\phi, kr\mu\right)\,. \tag{40}$$

We calculate the linear matter power spectrum $P_{11}(k)$ from `CAMB` code with cosmological parameters given in Table 1 of [24]. We find that setting the radial integral range for r from $r_{\rm min}=10^{-2}k_H/k$ to $r_{\rm max}=10^6k_H/k$ is sufficient to guarantee the convergence. All results we show hereafter are for $z=0$.

In Figure 1 we show the matter bispectrum $B_{\rm total}$ up to one-loop corrections as well as individual component: leading order $B_{\rm tree}$, Newtonian one-loop $B^{\rm NT}_{1-\rm loop}$, relativistic one-loop $B^{\rm GR}_{1-\rm loop}$ and their sum $B^{\rm NT+GR}_{1-\rm loop}$. For each curve, dashes lines show the absolute value of the negative quantity. The Newtonian one-loop corrections are appreciable on sub-horizon scales, $k\gtrsim0.1h{\rm Mpc}^{-1}$, and dominates the tree contribution for large k indicating the strong non-linearities due to gravitational instability. They change sign at around $k\sim0.1h{\rm Mpc}^{-1}$, and on smaller (larger) scales the Newtonian corrections are negative (positive). The general relativistic one-loop corrections are strongly suppressed on small scales, but we note that on very large scales ($k\to0$ limit) they approach a constant value. While sub-dominant on all scales in the equilateral and folded configurations, the

relativistic corrections give rise to the notable changes to the matter bispectrum on large scales for more squeezed triangles. In the tightly squeezed limit ($\alpha = 100$) they even dominate the tree contribution and make the total bispectrum negative, i.e. anti-correlated. This peculiar behavior is mainly coming from the components that carry k_H^4 factor in the fourth order kernel F_4.

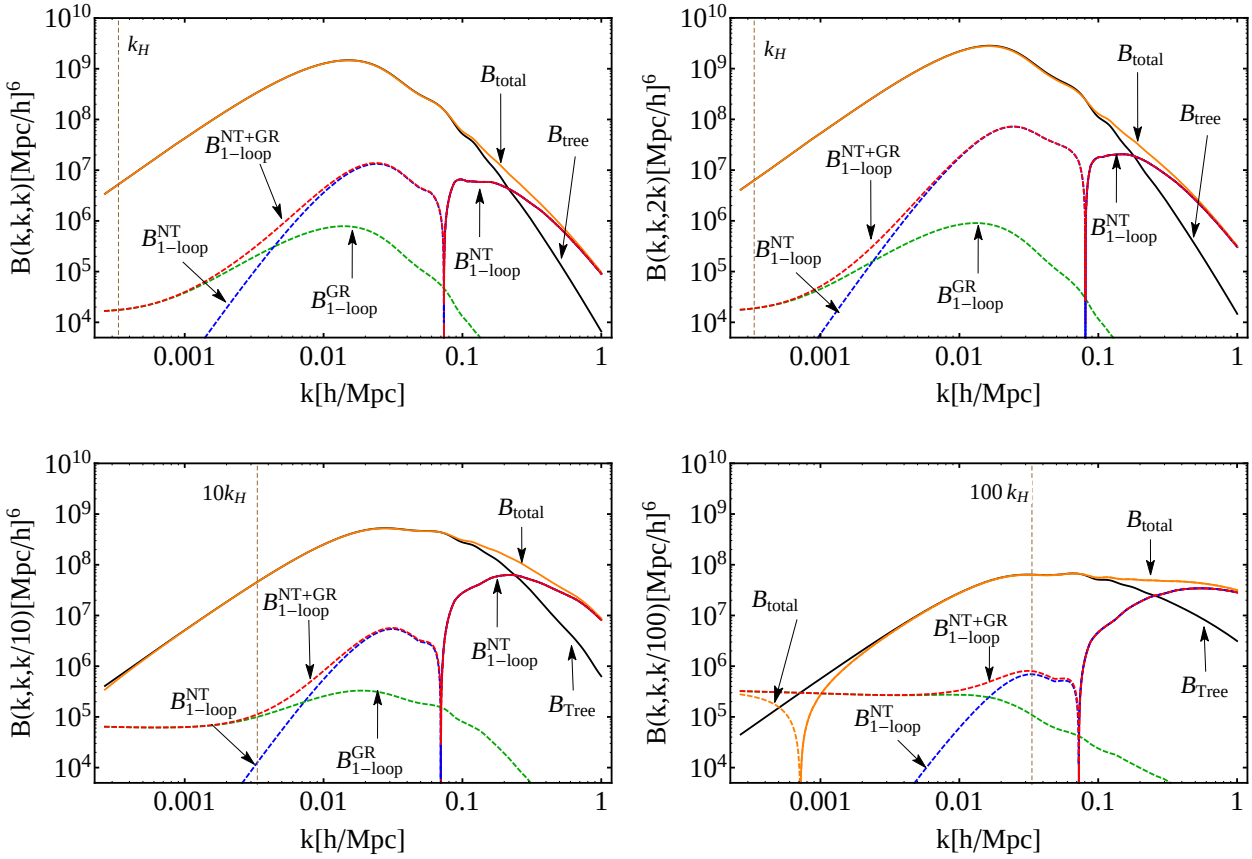

Figure 1: In each panel, we present the matter density bispectrum in the (clockwise from top left) equilateral, folded, tightly ($\alpha = 100$) and slightly ($\alpha = 10$) squeezed configuration at $z = 0$. Solid (dashed) lines indicate that the corresponding contributions have positive (negative) values. The vertical dotted line denotes the Hubble horizon scale k_H.

We estimate the behavior of the large scale plateau as the following. For simplicity, let us abbreviate the radial integration with the k_H^4 factor of F_4 in $B^{(1)}_{114}(k, k, k/\alpha)$ as $\int dr P_{11}(kr) f(r)$. The variable $r \equiv q/k$ is very large on large scale since $k \to 0$. With this, we can understand the asymptotic behavior of $f(r)$ on large scale ($r \gg 1$) and in the squeezed limit ($\alpha \gg 1$) as

$$f(r) = -\frac{75 k_H^4}{28\pi^2 k} \alpha^2 P_{11}(k) P_{11}\left(\frac{k}{\alpha}\right) + \mathcal{O}(r^{-2})\,. \tag{41}$$

Note that $f(r)$ is to leading order independent of r in the large scale limit. Using the fact $P_{11}(k) \propto k^{n_{\mathcal{R}}}$ for small k with $n_{\mathcal{R}} \sim 0.96$ being the spectral index of the primordial perturbation, we can simply write the squeezed bispectrum on very large scales as

$$B^{(1)}_{114}(k, k, k/\alpha) \propto -\frac{75 k_H^4}{28\pi^2} \alpha k^{2(n_{\mathcal{R}}-1)}\,. \tag{42}$$

Therefore, the matter bispectrum in the squeezed configuration is proportional to α and is nearly independent of k.

We show in Figure 2 the velocity bispectrum. The non-linear velocity bispectrum shows the similar features as the density bispectrum in Figure 1. Especially, the plateau on large scales in the squeezed configuration can be estimated in a similar way: writing the relevant component from G_4 schematically as $k_H^3 \int dr P_{11}(kr) g(r)$, in the large scale limit we can find $g(r) = f(r)/3$. Note, however, that the magnitude is much smaller than the matter bispectrum, due to the suppression by a factor of k_H^3.

As we see from both figures, the relativistic corrections to the density and velocity bispectra are very well-regulated, as the general relativistic signature shows only with a small amplitude on smaller scales and is noticible only for the large scale where the smallest mode is beyond the horizon scale, $k_H = aH$, shown as a vertical dashed line in the figures.

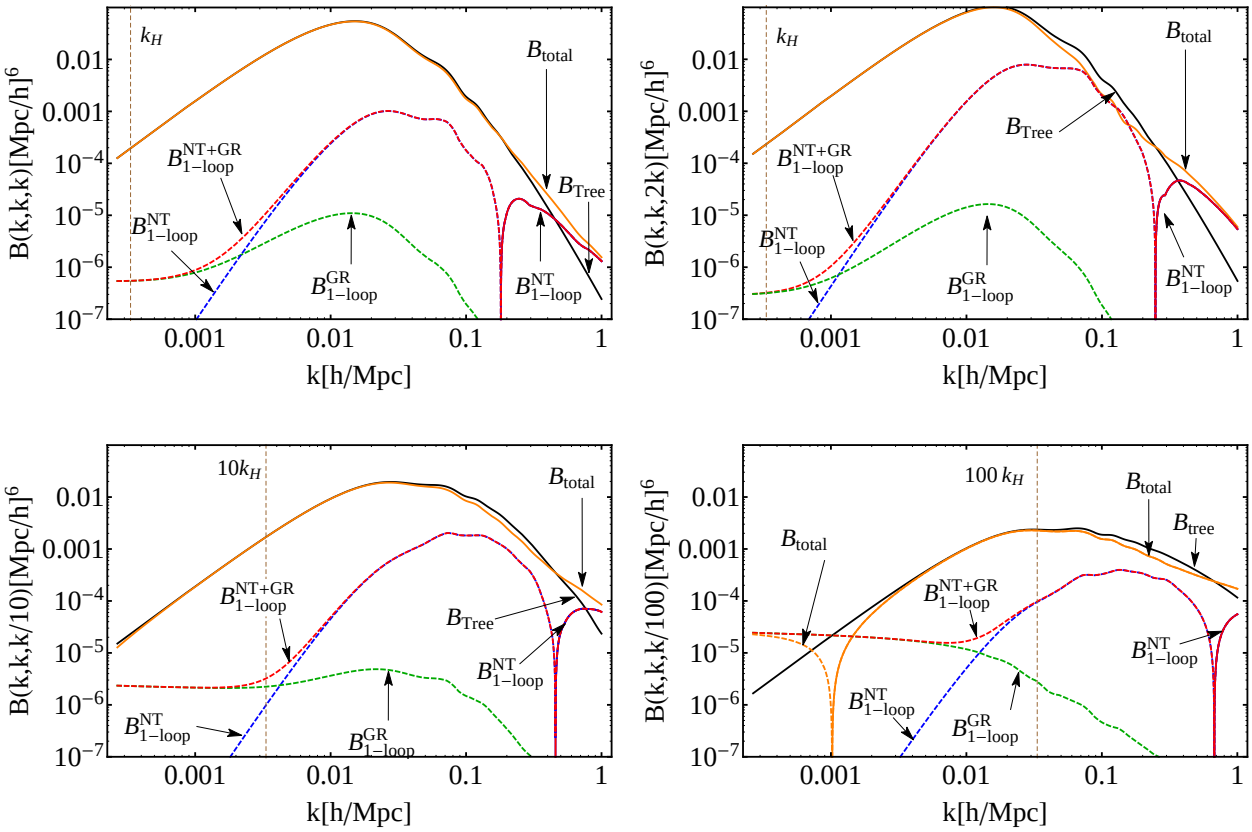

Figure 2: Velocity bispectrum shown in the same manner as Figure 1.

5 Tree bispectrum in other gauges

As we have seen above, the matter and velocity bispectra are well-regulated on all scales, and the relativistic effects are noticeable only on large scales beyond the horizon scale. This is because the comoving gauge is privileged in such a way that we have the same results as the Newtonian calculation up to second order. However, in other gauges this is not guaranteed and we in general expect deviations from each other, especially on large scales. To illustrate this point, we show in a few popular gauges the tree level bispectrum for which we need second order perturbation δ_2, or equivalently, second order kernel F_2. Note that, while we calculate the second order solutions with various gauge choices, the second order kernels F_2 we present here are still defined in Eq. (21) with the linear density contrast in the comoving gauge that we are referring as δ_1 throughout this paper.

- Comoving gauge: This is the main gauge we work with in this article. As we have worked out in the

previous section, δ_1 and δ_2 are identical to the Newtonian density perturbations in the Eulerian coordinate. Thus there is no relativistic contributions at tree level.

- Synchronous gauge: Synchronous gauge takes no perturbation in the 00 and $0i$ components of the metric,

$$ds^2 = -dt^2 + a^2(1+2\varphi)\delta_{ij}dx^i dx^j\,, \tag{43}$$

so that the time coordinate agrees with proper time. In this gauge δ_1 is the same as that in the comoving gauge, but the second order kernel is found to be

$$F_2^{(\mathrm{sg})}(\boldsymbol{q}_1,\boldsymbol{q}_2) = \frac{5}{7} + \frac{2}{7}\frac{(\boldsymbol{q}_1\cdot\boldsymbol{q}_2)^2}{q_1^2 q_2^2}\,. \tag{44}$$

Thus although there is no divergence on large scales, the tree bispectrum does not match that in the comoving gauge everywhere. This is because the density field in the synchronous gauge can be interpreted as the Newtonian density perturbation in the Lagrangian point of view following the moving volume elements.

- Zero shear gauge: In this gauge the metric is written as

$$ds^2 = -(1+2\Phi)dt^2 + a^2(1-2\Psi)\delta_{ij}dx^i dx^j\,. \tag{45}$$

We find the linear perturbation is given by

$$\delta_1^{(\mathrm{zsg})}(\boldsymbol{k}) = \left(1+\frac{3k_H^2}{k^2}\right)\delta_1(\boldsymbol{k})\,. \tag{46}$$

Thus, while we recover the same result on sub-horizon scales as in the comoving gauge, deviation becomes prominent as we approach the horizon scale and eventually we face divergence on super-horizon scales. We can find the second order kernel as

$$\begin{aligned} F_2{}^{(\mathrm{zsg})}(\boldsymbol{q}_1,\boldsymbol{q}_2) &= F_2^{(\mathrm{cg})}(\boldsymbol{q}_1,\boldsymbol{q}_2) \\ &+ \left(\frac{k_H}{k}\right)^2\left[\frac{9}{7} + \frac{q_{12}^2}{q_1^2} + \frac{q_{12}^2}{q_2^2} + \frac{12\,(\boldsymbol{q}_1\cdot\boldsymbol{q}_2)^2}{7q_1^2q_2^2} + \frac{3\boldsymbol{q}_1\cdot\boldsymbol{q}_2}{2q_1^2} + \frac{3\boldsymbol{q}_1\cdot\boldsymbol{q}_2}{2q_2^2}\right] \\ &+ \left(\frac{k_H}{k}\right)^4\left[\frac{105}{4} - \frac{15\,(\boldsymbol{q}_1\cdot\boldsymbol{q}_2)^2}{4q_1^2q_2^2} + \frac{75\boldsymbol{q}_1\cdot\boldsymbol{q}_2}{4q_1^2} + \frac{75\boldsymbol{q}_1\cdot\boldsymbol{q}_2}{4q_2^2} + \frac{15q_2^2}{2q_1^2} + \frac{15q_1^2}{2q_2^2} + \frac{9q_{12}^4}{2q_1^2q_2^2} + \frac{3q_{12}^2\boldsymbol{q}_1\cdot\boldsymbol{q}_2}{2q_1^2q_2^2}\right]. \end{aligned} \tag{47}$$

This also matches the comoving gauge kernel on small scales but diverges in the limit $k\to 0$. The relativistic effect of gauge dependence in this gauge is characterized by the second and the third terms in the kernel with a factor of k_H.

- Uniform curvature gauge: This gauge is also called as the flat gauge. In this gauge the spatial metric is set to be unperturbed,

$$ds^2 = -(1+2A)dt^2 - 2B_i dx^i dt + a^2\delta_{ij}dx^i dx^j\,. \tag{48}$$

The linear perturbation in this gauge is

$$\delta_1^{(\mathrm{ucg})}(\boldsymbol{k}) = \left(1+\frac{15k_H^2}{2k^2}\right)\delta_1(\boldsymbol{k})\,, \tag{49}$$

thus as in the zero shear gauge we find divergence on large scales. The second order kernel is given by

$$\begin{aligned} F_2^{(\mathrm{ucg})}(\boldsymbol{q}_1,\boldsymbol{q}_2) =& F_2^{(\mathrm{cg})}(\boldsymbol{q}_1,\boldsymbol{q}_2) \\ &+ \left(\frac{k_H}{k}\right)^2\left[\frac{15}{4} + \frac{5q_{12}^2}{2q_1^2} + \frac{5q_{12}^2}{2q_2^2} + \frac{15\,(\boldsymbol{q}_1\cdot\boldsymbol{q}_2)^2}{4q_1^2q_2^2} + \frac{15\boldsymbol{q}_1\cdot\boldsymbol{q}_2}{4q_1^2} + \frac{15\boldsymbol{q}_1\cdot\boldsymbol{q}_2}{4q_2^2}\right] \\ &+ \left(\frac{k_H}{k}\right)^4\left(\frac{225q_{12}^2\boldsymbol{q}_1\cdot\boldsymbol{q}_2}{8q_1^2q_2^2} + \frac{75q_{12}^2}{2q_1^2} + \frac{75q_{12}^2}{2q_2^2} + \frac{75q_{12}^4}{8q_1^2q_2^2}\right). \end{aligned} \tag{50}$$

Likewise, we recover the comoving gauge result on small scales $k\to\infty$.

We compare the tree level bispectra in all the aforementioned gauges in Figure 3. On small scales, the tree-level bispectra from all gauges except for the synchronous gauge converge to the Newtonian tree level bispectrum: the bispectrum in the synchronous gauge does not converge to the Newtonian (Eulerian) bispectrum, because the coordinate system is the similar to the Lagrangian fluid view. On larger scales ($k_3 \lesssim k_H$), we start to see the gauge dependence of the matter density fields and the tree level bispectra from all four gauges are different from each other.

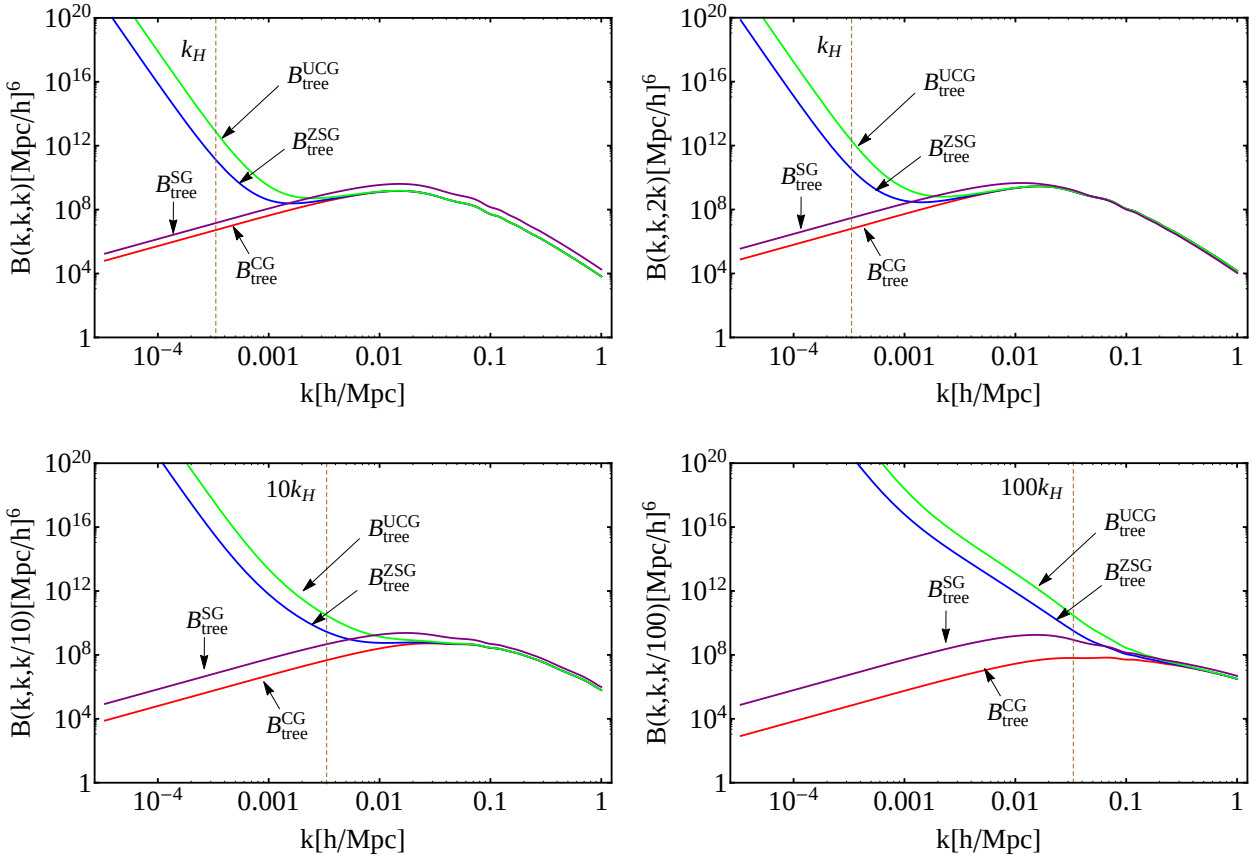

Figure 3: We show the tree bispectrum in the comoving (CG), synchronous (SG), zero shear (ZSG) and uniform curvature (UCG) gauges. From top left clockwise, the bispectra are projected onto the equilateral, folded, tightly ($\alpha = 100$) and slightly ($\alpha = 10$) squeezed configurations at $z = 0$.

6 Conclusions

We have studied how the non-linearities in general relativistic affects the non-linear density and velocity bispectra. Using the full general relativistic formalism, we calculate one-loop bispectra of density and velocity fields in a flat, matter dominated universe. We have assumed that the initial density perturbation is perfectly Gaussian, so that the matter bispectrum comes solely from the non-linear dynamics. As we work in the comoving gauge, where the relativistic density and velocity fields coincide with those in the Newtonian theory, the pure relativistic corrections appear from third order. We have computed the non-linear bispectrum in the equilateral, folded and squeezed triangular configurations and have shown that the relativistic effects are appreciable only on the scale larger than the horizon. On small scales, the Newtonian one-loop corrections dominate the relativistic ones and even the tree contributions at $k \gtrsim 0.2h\mathrm{Mpc}^{-1}$, indicating the non-linear evolution of the bispectrum due to gravitational instability. The general relativistic corrections appear to be dominant over the Newtonian ones when the longest wavemode is near comoving horizon scale. That is the reason why we see the domination of the relativistic corrections in the squeezed configurations on very large scales.

We then have demonstrated the gauge dependence of the matter bispectrum by explicitly computing the tree-level matter bispectrum in four different gauges: comoving, synchronous, zero shear and uniform curvature gauges. Except for the synchronous gauge, whose time coordinate is comoving with the observer and thus the meaning of the density contrast differs from the other gauges even on the small scales, the matter bispectrum computed in the other gauges are the same on small scales. On large scales, the gauge dependence begin to show up more prominently and the matter bisepctra from all four gauges diverge from each other. This result is, again, consistent with the one-loop result in the comoving gauge that the general relativistic effects are only important near the horizon scales.

The gauge dependence that we see near the horizon scale is the outcome of that the matter bispectrum itself is not a direct observable. When considering the observable quantities such as the bispectrum of weak-lensing shear and convergence field, or the galaxy bispectrum including all the relevant effects such as galaxy bias, light reflection, etc, the gauge dependence must disappear. In the case of the galaxy power spectrum, [19] have shown that the observed galaxy power spectrum written in terms of the observed coordinate system is indeed gauge independent. Likewise, we surmise that calculating the bispectrum of observed quantities should resolve this gauge dependent ambiguities. Such a calculation requires extending the previous work done for the galaxy power spectrum to second order.

Acknowledgements

SGB appreciates Jai-chan Hwang for suggesting helpful comments and supporting this research. We thank the Topical Research Program "Theories and practices in large scale structure formation", supported by the Asia Pacific Center for Theoretical Physics, while this work was under progress. JG acknowledges the Max-Planck-Gesellschaft, the Korea Ministry of Education, Science and Technology, Gyeongsangbuk-Do and Pohang City for the support of the Independent Junior Research Group at the Asia Pacific Center for Theoretical Physics. JG is also supported by a Starting Grant through the Basic Science Research Program of the National Research Foundation of Korea (2013R1A1A1006701). DJ is supported by DoE SC-0008108 and NASA NNX12AE86G, and acknowledges support from the John Templeton Foundation.

A Fourth order solutions

Substituting (21) and (22) into (13) and (14), in Fourier space we obtain the differential equations for the fourth order kernels F_4 and G_4 as

$$
\begin{aligned}
&\frac{1}{H}\frac{dF_4}{dt}+4F_4-G_4\\
=&\frac{\boldsymbol{k}\cdot\boldsymbol{q}_{234}}{q_{234}^2}G_3(\boldsymbol{q}_2,\boldsymbol{q}_3,\boldsymbol{q}_4)+\frac{\boldsymbol{k}\cdot\boldsymbol{q}_{34}}{q_{34}^2}F_2(\boldsymbol{q}_1,\boldsymbol{q}_2)G_2(\boldsymbol{q}_3,\boldsymbol{q}_4)+\frac{\boldsymbol{k}\cdot\boldsymbol{q}_1}{q_1^2}F_3(\boldsymbol{q}_2,\boldsymbol{q}_3,\boldsymbol{q}_4)\\
&-(aH)^2\Bigg\{\frac{5}{2}\Bigg[\frac{\boldsymbol{q}_{12}\cdot\boldsymbol{q}_{34}}{q_{12}^2}\Bigg(-\frac{2}{q_2^2}+\frac{\boldsymbol{q}_1\cdot\boldsymbol{q}_2}{q_1^2q_2^2}-\frac{3}{2}\frac{\boldsymbol{q}_{12}\cdot\boldsymbol{q}_1}{q_{12}^2q_1^2}-\frac{3}{2}\frac{\boldsymbol{q}_{12}\cdot\boldsymbol{q}_2}{q_{12}^2}\frac{\boldsymbol{q}_1\cdot\boldsymbol{q}_2}{q_1^2q_2^2}\Bigg)+2\frac{\boldsymbol{q}_1\cdot\boldsymbol{q}_{34}}{q_1^2q_2^2}\Bigg]F_2(\boldsymbol{q}_3,\boldsymbol{q}_4)\\
&\quad+\Bigg[\frac{\boldsymbol{q}_{123}\cdot\boldsymbol{q}_4}{q_{123}^2}\Bigg(-\frac{2}{q_{23}^2}+\frac{\boldsymbol{q}_1\cdot\boldsymbol{q}_{23}}{q_1^2q_{23}^2}-\frac{3}{2}\frac{\boldsymbol{q}_{123}\cdot\boldsymbol{q}_1}{q_{123}^2q_1^2}-\frac{3}{2}\frac{\boldsymbol{q}_{123}\cdot\boldsymbol{q}_{23}}{q_{123}^2}\frac{\boldsymbol{q}_1\cdot\boldsymbol{q}_{23}}{q_1^2q_{23}^2}\Bigg)+2\frac{\boldsymbol{q}_1\cdot\boldsymbol{q}_4}{q_1^2q_{23}^2}\Bigg]\Bigg[\frac{3}{2}F_2(\boldsymbol{q}_2,\boldsymbol{q}_3)+G_2(\boldsymbol{q}_2,\boldsymbol{q}_3)\Bigg]\\
&\quad+\frac{5}{2}\Bigg[\frac{\boldsymbol{q}_{123}\cdot\boldsymbol{q}_4}{q_{123}^2}\Bigg(-\frac{2}{q_1^2}+\frac{\boldsymbol{q}_1\cdot\boldsymbol{q}_{23}}{q_1^2q_{23}^2}-\frac{3}{2}\frac{\boldsymbol{q}_{123}\cdot\boldsymbol{q}_{23}}{q_{123}^2q_{23}^2}-\frac{3}{2}\frac{\boldsymbol{q}_{123}\cdot\boldsymbol{q}_1}{q_{123}^2}\frac{\boldsymbol{q}_1\cdot\boldsymbol{q}_{23}}{q_1^2q_{23}^2}\Bigg)+2\frac{\boldsymbol{q}_{23}\cdot\boldsymbol{q}_4}{q_1^2q_{23}^2}\Bigg]G_2(\boldsymbol{q}_2,\boldsymbol{q}_3)\Bigg\}\\
&+\frac{\boldsymbol{q}_1\cdot\boldsymbol{q}_{234}}{q_{234}^2}\Bigg\{\frac{25}{4}(aH)^4\Bigg(\frac{2}{q_4^2}-\frac{\boldsymbol{q}_{23}\cdot\boldsymbol{q}_4}{q_{23}^2q_4^2}+\frac{3}{2}\frac{\boldsymbol{q}_{234}\cdot\boldsymbol{q}_{23}}{q_{234}^2q_{23}^2}+\frac{3}{2}\frac{\boldsymbol{q}_{234}\cdot\boldsymbol{q}_4}{q_{234}^2}\frac{\boldsymbol{q}_{23}\cdot\boldsymbol{q}_4}{q_{23}^2q_4^2}\Bigg)\\
&\quad+\frac{(aH)^2}{2q_{34}^2}\Bigg(-2+\frac{\boldsymbol{q}_2\cdot\boldsymbol{q}_{34}}{q_2^2}-\frac{3}{2}\frac{\boldsymbol{q}_{234}\cdot\boldsymbol{q}_2}{q_{234}^2}\frac{q_{34}^2}{q_2^2}-\frac{3}{2}\frac{\boldsymbol{q}_{234}\cdot\boldsymbol{q}_{34}}{q_{234}^2}\frac{\boldsymbol{q}_2\cdot\boldsymbol{q}_{34}}{q_{34}^2}\Bigg)\\
&\qquad\times\Bigg\{\frac{1}{2}\Bigg[1+\frac{\boldsymbol{q}_3\cdot\boldsymbol{q}_4}{q_3^2}\Bigg(1-\frac{\boldsymbol{q}_{34}\cdot\boldsymbol{q}_4}{q_4^2}\Bigg)\Bigg]-\frac{25}{4}\frac{(aH)^2}{q_3^2q_4^2}\left(3\boldsymbol{q}_3\cdot\boldsymbol{q}_4+8q_4^2\right)\Bigg\}\\
&\quad+\frac{25}{4}\frac{(aH)^4}{q_3^2q_4^2}\Bigg[-4+4\frac{\boldsymbol{q}_2\cdot\boldsymbol{q}_3}{q_2^2}-\frac{3}{2}\Bigg(\frac{\boldsymbol{q}_{234}\cdot\boldsymbol{q}_2}{q_{234}^2}\frac{\boldsymbol{q}_3\cdot\boldsymbol{q}_4}{q_2^2}+3\frac{\boldsymbol{q}_{234}\cdot\boldsymbol{q}_4}{q_{234}^2}\frac{\boldsymbol{q}_2\cdot\boldsymbol{q}_3}{q_2^2}+4\frac{\boldsymbol{q}_{234}\cdot\boldsymbol{q}_3}{q_{234}^2}\frac{\boldsymbol{q}_2\cdot\boldsymbol{q}_3}{q_2^2}+4\frac{\boldsymbol{q}_{234}\cdot\boldsymbol{q}_2}{q_{234}^2}\frac{q_3^2}{q_2^2}\Bigg)\Bigg]\Bigg\}\\
&+2\Bigg\{\frac{\boldsymbol{q}_1\cdot\boldsymbol{q}_2}{2q_2^2q_{34}^2}\Bigg(\frac{(aH)^2}{2}\Bigg[1+\frac{\boldsymbol{q}_3\cdot\boldsymbol{q}_4}{q_3^2}\Bigg(1-\frac{\boldsymbol{q}_{34}\cdot\boldsymbol{q}_4}{q_4^2}\Bigg)\Bigg]-\frac{25}{4}\frac{(aH)^4}{q_3^2q_4^2}\left(3\boldsymbol{q}_3\cdot\boldsymbol{q}_4+8q_4^2\right)\Bigg)\\
&\quad+\frac{25}{4}\frac{(aH)^4}{q_2^2}\frac{\boldsymbol{q}_1\cdot\boldsymbol{q}_{34}}{q_{34}^2}\Bigg[-\frac{2}{q_4^2}+\frac{\boldsymbol{q}_3\cdot\boldsymbol{q}_4}{q_3^2q_4^2}-\frac{3}{2}\frac{\boldsymbol{q}_{34}\cdot\boldsymbol{q}_3}{q_{34}^2q_3^2}-\frac{3}{2}\frac{\boldsymbol{q}_{34}\cdot\boldsymbol{q}_4}{q_{34}^2}\frac{\boldsymbol{q}_3\cdot\boldsymbol{q}_4}{q_3^2q_4^2}\Bigg]\Bigg\}-25\frac{\boldsymbol{q}_1\cdot\boldsymbol{q}_2}{q_2^2}\frac{(aH)^4}{q_3^2q_4^2}\,,
\end{aligned}
\tag{51}
$$

and

$$
\begin{aligned}
&\frac{1}{H}\frac{dG_4}{dt}+\frac{3}{2}\left(3G_4-F_4\right)\\
=&\frac{k^2\boldsymbol{q}_1\cdot\boldsymbol{q}_{234}}{q_1^2q_{234}^2}G_3(\boldsymbol{q}_2,\boldsymbol{q}_3,\boldsymbol{q}_4)+\frac{k^2\boldsymbol{q}_{12}\cdot\boldsymbol{q}_{34}}{2q_{12}^2q_{34}^2}G_2(\boldsymbol{q}_1,\boldsymbol{q}_2)G_2(\boldsymbol{q}_3,\boldsymbol{q}_4)\\
&+(aH)^2\Bigg(\Bigg\{\left[\frac{2}{3}+\frac{\boldsymbol{q}_1\cdot\boldsymbol{q}_{234}}{q_1^2}\left(1-\frac{k^2}{q_{234}^2}\right)\right]\left(-\frac{2}{q_2^2}+\frac{\boldsymbol{q}_2\cdot\boldsymbol{q}_{34}}{q_2^2q_{34}^2}-\frac{3}{2}\frac{\boldsymbol{q}_{234}\cdot\boldsymbol{q}_{34}}{q_{234}^2q_{34}^2}-\frac{3}{2}\frac{\boldsymbol{q}_{234}\cdot\boldsymbol{q}_2}{q_{234}^2}\frac{\boldsymbol{q}_2\cdot\boldsymbol{q}_{34}}{q_2^2q_{34}^2}\right)\\
&\quad+\frac{1}{q_2^2}\left[\frac{2}{3}\frac{\boldsymbol{q}_1\cdot\boldsymbol{q}_{34}}{q_{34}^2}-4\left(\frac{\boldsymbol{q}_1\cdot\boldsymbol{q}_{34}}{q_{34}^2}-\frac{1}{3}\right)\frac{\boldsymbol{k}\cdot\boldsymbol{q}_1}{q_1^2}\right]\Bigg\}\frac{5}{2}G_2(\boldsymbol{q}_3,\boldsymbol{q}_4)\\
&\qquad+\Bigg\{\left[\frac{2}{3}+\frac{\boldsymbol{q}_{12}\cdot\boldsymbol{q}_{34}}{q_{34}^2}\left(1-\frac{k^2}{q_{12}^2}\right)\right]\left(-\frac{2}{q_2^2}+\frac{\boldsymbol{q}_1\cdot\boldsymbol{q}_2}{q_1^2q_2^2}-\frac{3}{2}\frac{\boldsymbol{q}_{12}\cdot\boldsymbol{q}_1}{q_{12}^2q_1^2}-\frac{3}{2}\frac{\boldsymbol{q}_{12}\cdot\boldsymbol{q}_2}{q_{12}^2}\frac{\boldsymbol{q}_1\cdot\boldsymbol{q}_2}{q_1^2q_2^2}\right)\\
&\qquad\quad+\frac{1}{q_2^2}\left[\frac{2}{3}\frac{\boldsymbol{q}_1\cdot\boldsymbol{q}_{34}}{q_1^2}-4\left(\frac{\boldsymbol{q}_1\cdot\boldsymbol{q}_{34}}{q_1^2}-\frac{1}{3}\right)\frac{\boldsymbol{k}\cdot\boldsymbol{q}_{34}}{q_{34}^2}\right]\Bigg\}\frac{5}{2}G_2(\boldsymbol{q}_3,\boldsymbol{q}_4)\\
&\qquad+\Bigg\{\left[\frac{2}{3}+\frac{\boldsymbol{q}_1\cdot\boldsymbol{q}_{234}}{q_1^2}\left(1-\frac{k^2}{q_{234}^2}\right)\right]\left(-\frac{2}{q_{34}^2}+\frac{\boldsymbol{q}_2\cdot\boldsymbol{q}_{34}}{q_2^2q_{34}^2}-\frac{3}{2}\frac{\boldsymbol{q}_2\cdot\boldsymbol{q}_{234}}{q_2^2q_{234}^2}-\frac{3}{2}\frac{\boldsymbol{q}_{234}\cdot\boldsymbol{q}_{34}}{q_{234}^2}\frac{\boldsymbol{q}_2\cdot\boldsymbol{q}_{34}}{q_2^2q_{34}^2}\right)\\
&\qquad\quad+\frac{1}{q_{34}^2}\left[\frac{2}{3}\frac{\boldsymbol{q}_1\cdot\boldsymbol{q}_2}{q_2^2}-4\left(\frac{\boldsymbol{q}_1\cdot\boldsymbol{q}_2}{q_2^2}-\frac{1}{3}\right)\frac{\boldsymbol{k}\cdot\boldsymbol{q}_1}{q_1^2}\right]\Bigg\}\left[\frac{3}{2}F_2(\boldsymbol{q}_3,\boldsymbol{q}_4)+G_2(\boldsymbol{q}_3,\boldsymbol{q}_4)\right]\Bigg)\\
&+\left(-\frac{2}{3}-\frac{\boldsymbol{q}_1\cdot\boldsymbol{q}_{234}}{q_1^2}+\frac{k^2}{q_{234}^2}\frac{\boldsymbol{q}_1\cdot\boldsymbol{q}_{234}}{q_1^2}\right)\\
&\quad\times\Bigg\{\frac{25}{4}(aH)^4\left(\frac{2}{q_4^2}-\frac{\boldsymbol{q}_{23}\cdot\boldsymbol{q}_4}{q_{23}^2q_4^2}+\frac{3}{2}\frac{\boldsymbol{q}_{234}\cdot\boldsymbol{q}_{23}}{q_{234}^2q_{23}^2}+\frac{3}{2}\frac{\boldsymbol{q}_{234}\cdot\boldsymbol{q}_4}{q_{234}^2}\frac{\boldsymbol{q}_{23}\cdot\boldsymbol{q}_4}{q_{23}^2q_4^2}\right)\\
&\qquad\qquad\times\left(\frac{2}{q_3^2}-\frac{\boldsymbol{q}_2\cdot\boldsymbol{q}_3}{q_2^2q_3^2}+\frac{3}{2}\frac{\boldsymbol{q}_{23}\cdot\boldsymbol{q}_2}{q_{23}^2q_2^2}+\frac{3}{2}\frac{\boldsymbol{q}_{23}\cdot\boldsymbol{q}_3}{q_{23}^2}\frac{\boldsymbol{q}_2\cdot\boldsymbol{q}_3}{q_2^2q_3^2}\right)\\
&\qquad+\frac{(aH)^2}{2q_{34}^2}\left(-2+\frac{\boldsymbol{q}_2\cdot\boldsymbol{q}_{34}}{q_2^2}-\frac{3}{2}\frac{\boldsymbol{q}_{234}\cdot\boldsymbol{q}_2}{q_{234}^2}\frac{q_{34}^2}{q_2^2}-\frac{3}{2}\frac{\boldsymbol{q}_{234}\cdot\boldsymbol{q}_{34}}{q_{234}^2}\frac{\boldsymbol{q}_2\cdot\boldsymbol{q}_{34}}{q_{34}^2}\right)\\
&\qquad\qquad\times\left\{\frac{1}{2}\left[1+\frac{\boldsymbol{q}_3\cdot\boldsymbol{q}_4}{q_3^2}\left(1-\frac{\boldsymbol{q}_{34}\cdot\boldsymbol{q}_4}{q_4^2}\right)\right]-\frac{25}{4}\frac{(aH)^2}{q_3^2q_4^2}\left(3\boldsymbol{q}_3\cdot\boldsymbol{q}_4+8q_4^2\right)\right\}\\
&\qquad+\frac{25}{4}\frac{(aH)^4}{q_3^2q_4^2}\left[-4+4\frac{\boldsymbol{q}_2\cdot\boldsymbol{q}_3}{q_2^2}-\frac{3}{2}\left(\frac{\boldsymbol{q}_{234}\cdot\boldsymbol{q}_2}{q_{234}^2}\frac{\boldsymbol{q}_3\cdot\boldsymbol{q}_4}{q_2^2}+3\frac{\boldsymbol{q}_{234}\cdot\boldsymbol{q}_4}{q_{234}^2}\frac{\boldsymbol{q}_2\cdot\boldsymbol{q}_3}{q_2^2}+4\frac{\boldsymbol{q}_{234}\cdot\boldsymbol{q}_3}{q_{234}^2}\frac{\boldsymbol{q}_2\cdot\boldsymbol{q}_3}{q_2^2}+4\frac{\boldsymbol{q}_{234}\cdot\boldsymbol{q}_2}{q_{234}^2}\frac{q_3^2}{q_2^2}\right)\right]\Bigg\}\\
&+\frac{(aH)^2}{2q_{34}^2}\left(-\frac{2}{3}\frac{\boldsymbol{q}_1\cdot\boldsymbol{q}_2}{q_1^2}+4\frac{\boldsymbol{q}_1\cdot\boldsymbol{q}_2}{q_1^2}\frac{\boldsymbol{k}\cdot\boldsymbol{q}_2}{q_2^2}-\frac{4}{3}\frac{\boldsymbol{k}\cdot\boldsymbol{q}_2}{q_2^2}\right)\\
&\qquad\qquad\times\left\{\frac{1}{2}\left[1+\frac{\boldsymbol{q}_3\cdot\boldsymbol{q}_4}{q_3^2}\left(1-\frac{\boldsymbol{q}_{34}\cdot\boldsymbol{q}_4}{q_4^2}\right)\right]-\frac{25}{4}\frac{(aH)^2}{q_3^2q_4^2}\left(3\boldsymbol{q}_3\cdot\boldsymbol{q}_4+8q_4^2\right)\right\}\\
&+\frac{25}{4}\frac{(aH)^4}{q_1^2}\left(-\frac{2}{q_4^2}+\frac{\boldsymbol{q}_3\cdot\boldsymbol{q}_4}{q_3^2q_4^2}-\frac{3}{2}\frac{\boldsymbol{q}_{34}\cdot\boldsymbol{q}_3}{q_{34}^2q_3^2}-\frac{3}{2}\frac{\boldsymbol{q}_{34}\cdot\boldsymbol{q}_4}{q_{34}^2}\frac{\boldsymbol{q}_3\cdot\boldsymbol{q}_4}{q_3^2q_4^2}\right)\\
&\qquad\qquad\times\left(4\frac{\boldsymbol{k}\cdot\boldsymbol{q}_2}{q_2^2}\frac{\boldsymbol{q}_2\cdot\boldsymbol{q}_{34}}{q_{34}^2}-\frac{4}{3}\frac{\boldsymbol{k}\cdot\boldsymbol{q}_2}{q_2^2}+4\frac{\boldsymbol{k}\cdot\boldsymbol{q}_{34}}{q_{34}^2}\frac{\boldsymbol{q}_2\cdot\boldsymbol{q}_{34}}{q_2^2}-\frac{4}{3}\frac{\boldsymbol{k}\cdot\boldsymbol{q}_{34}}{q_{34}^2}-\frac{2}{3}\frac{\boldsymbol{q}_2\cdot\boldsymbol{q}_{34}}{q_{34}^2}-\frac{8}{3}\frac{\boldsymbol{q}_2\cdot\boldsymbol{q}_{34}}{{q_2}^2}\right)\\
&+\frac{25}{4}\frac{(aH)^4}{q_1^2q_2^2}\left(12\frac{\boldsymbol{q}_3\cdot\boldsymbol{q}_4}{q_3^2}\frac{\boldsymbol{k}\cdot\boldsymbol{q}_4}{q_4^2}-4\frac{\boldsymbol{k}\cdot\boldsymbol{q}_4}{q_4^2}-4\frac{\boldsymbol{q}_3\cdot\boldsymbol{q}_4}{q_3^2}+2\frac{\boldsymbol{q}_1\cdot\boldsymbol{q}_2}{q_3^2}\frac{\boldsymbol{q}_3\cdot\boldsymbol{q}_4}{q_4^2}+\frac{2}{3}\frac{\boldsymbol{q}_1\cdot\boldsymbol{q}_3}{q_3^2}\frac{\boldsymbol{q}_2\cdot\boldsymbol{q}_4}{q_4^2}\right)\\
&+\frac{25}{4}(aH)^4\left(\frac{2}{3}-\frac{\boldsymbol{k}\cdot\boldsymbol{q}_{34}}{q_{34}^2}+\frac{\boldsymbol{k}\cdot\boldsymbol{q}_{34}}{q_{34}^2}\frac{\boldsymbol{q}_{12}\cdot\boldsymbol{q}_{34}}{q_{12}^2}\right)\\
&\qquad\qquad\times\left(\frac{2}{q_2^2}-\frac{\boldsymbol{q}_1\cdot\boldsymbol{q}_2}{q_1^2q_2^2}+\frac{3}{2}\frac{\boldsymbol{q}_{12}\cdot\boldsymbol{q}_1}{q_{12}^2q_1^2}+\frac{3}{2}\frac{\boldsymbol{q}_{12}\cdot\boldsymbol{q}_2}{q_{12}^2}\frac{\boldsymbol{q}_1\cdot\boldsymbol{q}_2}{q_1^2q_2^2}\right)\left(\frac{2}{q_4^2}-\frac{\boldsymbol{q}_3\cdot\boldsymbol{q}_4}{q_3^2q_4^2}+\frac{3}{2}\frac{\boldsymbol{q}_{34}\cdot\boldsymbol{q}_3}{q_{34}^2q_3^2}+\frac{3}{2}\frac{\boldsymbol{q}_{34}\cdot\boldsymbol{q}_4}{q_{34}^2}\frac{\boldsymbol{q}_3\cdot\boldsymbol{q}_4}{q_3^2q_4^2}\right).
\end{aligned}
\tag{52}
$$

We can obtain readily the solutions of these equations. We can divide the kernels into the Newtonian and general relativistic parts. The Newtonian kernels are time independent, and can be calculated algebraically in

terms of lower order kernels as

$$F_4^{(\mathrm{N})} = \frac{1}{33}\left[\frac{9\boldsymbol{k}\cdot\boldsymbol{q}_1}{q_1^2}F_3^{(\mathrm{N})}(\boldsymbol{q}_2,\boldsymbol{q}_3,\boldsymbol{q}_4) + \frac{9\boldsymbol{k}\cdot\boldsymbol{q}_{234}}{q_{234}^2}G_3^{(\mathrm{N})}(\boldsymbol{q}_2,\boldsymbol{q}_3,\boldsymbol{q}_4) + \frac{9\boldsymbol{k}\cdot\boldsymbol{q}_{34}}{q_{34}^2}F_2(\boldsymbol{q}_1,\boldsymbol{q}_2)G_2(\boldsymbol{q}_3,\boldsymbol{q}_4)\right.$$
$$\left. + \frac{2k^2\boldsymbol{q}_1\cdot\boldsymbol{q}_{234}}{q_1^2 q_{234}^2}G_3^{(\mathrm{N})}(\boldsymbol{q}_2,\boldsymbol{q}_3,\boldsymbol{q}_4) + \frac{2k^2\boldsymbol{q}_{12}\cdot\boldsymbol{q}_{34}}{2q_{12}^2 q_{34}^2}G_2(\boldsymbol{q}_1,\boldsymbol{q}_2)G_2(\boldsymbol{q}_3,\boldsymbol{q}_4)\right], \tag{53}$$

$$G_4^{(\mathrm{N})} = \frac{1}{33}\left[\frac{3\boldsymbol{k}\cdot\boldsymbol{q}_1}{q_1^2}F_3^{(\mathrm{N})}(\boldsymbol{q}_2,\boldsymbol{q}_3,\boldsymbol{q}_4) + \frac{3\boldsymbol{k}\cdot\boldsymbol{q}_{234}}{q_{234}^2}G_3^{(\mathrm{N})}(\boldsymbol{q}_2,\boldsymbol{q}_3,\boldsymbol{q}_4) + \frac{3\boldsymbol{k}\cdot\boldsymbol{q}_{34}}{q_{34}^2}F_2(\boldsymbol{q}_1,\boldsymbol{q}_2)G_2(\boldsymbol{q}_3,\boldsymbol{q}_4)\right.$$
$$\left. + \frac{8k^2\boldsymbol{q}_1\cdot\boldsymbol{q}_{234}}{q_1^2 q_{234}^2}G_3^{(\mathrm{N})}(\boldsymbol{q}_2,\boldsymbol{q}_3,\boldsymbol{q}_4) + \frac{8k^2\boldsymbol{q}_{12}\cdot\boldsymbol{q}_{34}}{2q_{12}^2 q_{34}^2}G_2(\boldsymbol{q}_1,\boldsymbol{q}_2)G_2(\boldsymbol{q}_3,\boldsymbol{q}_4)\right]. \tag{54}$$

Meanwhile, the general relativistic kernels are time dependent. Introducing the horizon scale wavenumber $k_H \equiv aH$, we can find

$$F_4^{(\mathrm{GR})} = \frac{7A_1+2B_1}{18}k_H^2 + \frac{5A_2+2B_2}{7}k_H^4\,, \tag{55}$$

$$G_4^{(\mathrm{GR})} = \frac{A_1+2B_1}{6}k_H^2 + \frac{3A_2+4B_2}{7}k_H^4\,, \tag{56}$$

where

$$
\begin{aligned}
A_1 &= \frac{\boldsymbol{k}\cdot\boldsymbol{q}_1}{q_1^2}k_H^{-2}F_3^{(\mathrm{GR})}(\boldsymbol{q}_2,\boldsymbol{q}_3,\boldsymbol{q}_4)+\frac{\boldsymbol{k}\cdot\boldsymbol{q}_{234}}{q_{234}^2}k_H^{-2}G_3^{(\mathrm{GR})}(\boldsymbol{q}_2,\boldsymbol{q}_3,\boldsymbol{q}_4)\\
&-\frac{5}{2}\left[\frac{\boldsymbol{q}_{12}\cdot\boldsymbol{q}_{34}}{q_{12}^2}\left(-\frac{2}{q_2^2}+\frac{\boldsymbol{q}_1\cdot\boldsymbol{q}_2}{q_1^2q_2^2}-\frac{3}{2}\frac{\boldsymbol{q}_{12}\cdot\boldsymbol{q}_1}{q_{12}^2q_1^2}-\frac{3}{2}\frac{\boldsymbol{q}_{12}\cdot\boldsymbol{q}_2}{q_{12}^2}\frac{\boldsymbol{q}_1\cdot\boldsymbol{q}_2}{q_1^2q_2^2}\right)+2\frac{\boldsymbol{q}_1\cdot\boldsymbol{q}_{34}}{q_1^2q_2^2}\right]F_2(\boldsymbol{q}_3,\boldsymbol{q}_4)\\
&-\left[\frac{\boldsymbol{q}_{123}\cdot\boldsymbol{q}_4}{q_{123}^2}\left(-\frac{2}{q_{23}^2}+\frac{\boldsymbol{q}_1\cdot\boldsymbol{q}_{23}}{q_1^2q_{23}^2}-\frac{3}{2}\frac{\boldsymbol{q}_{123}\cdot\boldsymbol{q}_1}{q_{123}^2q_1^2}-\frac{3}{2}\frac{\boldsymbol{q}_{123}\cdot\boldsymbol{q}_{23}}{q_{123}^2}\frac{\boldsymbol{q}_1\cdot\boldsymbol{q}_{23}}{q_1^2q_{23}^2}\right)+2\frac{\boldsymbol{q}_1\cdot\boldsymbol{q}_4}{q_1^2q_{23}^2}\right]\left[\frac{3}{2}F_2(\boldsymbol{q}_2,\boldsymbol{q}_3)+G_2(\boldsymbol{q}_2,\boldsymbol{q}_3)\right]\\
&-\frac{5}{2}\left[\frac{\boldsymbol{q}_{123}\cdot\boldsymbol{q}_4}{q_{123}^2}\left(-\frac{2}{q_1^2}+\frac{\boldsymbol{q}_1\cdot\boldsymbol{q}_{23}}{q_1^2q_{23}^2}-\frac{3}{2}\frac{\boldsymbol{q}_{123}\cdot\boldsymbol{q}_{23}}{q_{123}^2q_{23}^2}-\frac{3}{2}\frac{\boldsymbol{q}_{123}\cdot\boldsymbol{q}_1}{q_{123}^2}\frac{\boldsymbol{q}_1\cdot\boldsymbol{q}_{23}}{q_1^2q_{23}^2}\right)+2\frac{\boldsymbol{q}_{23}\cdot\boldsymbol{q}_4}{q_1^2q_{23}^2}\right]G_2(\boldsymbol{q}_2,\boldsymbol{q}_3)\\
&+\frac{\boldsymbol{q}_1\cdot\boldsymbol{q}_{234}}{q_{234}^2}\frac{1}{4q_{34}^2}\left(-2+\frac{\boldsymbol{q}_2\cdot\boldsymbol{q}_{34}}{q_2^2}-\frac{3}{2}\frac{\boldsymbol{q}_{234}\cdot\boldsymbol{q}_2}{q_{234}^2}\frac{q_{34}^2}{q_2^2}-\frac{3}{2}\frac{\boldsymbol{q}_{234}\cdot\boldsymbol{q}_{34}}{q_{234}^2}\frac{\boldsymbol{q}_2\cdot\boldsymbol{q}_{34}}{q_{34}^2}\right)\left[1+\frac{\boldsymbol{q}_3\cdot\boldsymbol{q}_4}{q_3^2}\left(1-\frac{\boldsymbol{q}_{34}\cdot\boldsymbol{q}_4}{q_4^2}\right)\right]\\
&+\frac{\boldsymbol{q}_1\cdot\boldsymbol{q}_2}{2q_2^2q_{34}^2}\left[1+\frac{\boldsymbol{q}_3\cdot\boldsymbol{q}_4}{q_3^2}\left(1-\frac{\boldsymbol{q}_{34}\cdot\boldsymbol{q}_4}{q_4^2}\right)\right],
\end{aligned}
\tag{57}
$$

$$
\begin{aligned}
B_1 &= \frac{k^2\boldsymbol{q}_1\cdot\boldsymbol{q}_{234}}{q_1^2q_{234}^2}k_H^{-2}G_3^{(\mathrm{GR})}(\boldsymbol{q}_2,\boldsymbol{q}_3,\boldsymbol{q}_4)\\
&+\frac{5}{2}\left\{\left[\frac{2}{3}+\frac{\boldsymbol{q}_1\cdot\boldsymbol{q}_{234}}{q_1^2}\left(1-\frac{k^2}{q_{234}^2}\right)\right]\left(-\frac{2}{q_2^2}+\frac{\boldsymbol{q}_2\cdot\boldsymbol{q}_{34}}{q_2^2q_{34}^2}-\frac{3}{2}\frac{\boldsymbol{q}_{234}\cdot\boldsymbol{q}_{34}}{q_{234}^2q_{34}^2}-\frac{3}{2}\frac{\boldsymbol{q}_{234}\cdot\boldsymbol{q}_2}{q_{234}^2}\frac{\boldsymbol{q}_2\cdot\boldsymbol{q}_{34}}{q_2^2q_{34}^2}\right)\right.\\
&\qquad\left.+\frac{1}{q_2^2}\left[\frac{2}{3}\frac{\boldsymbol{q}_1\cdot\boldsymbol{q}_{34}}{q_{34}^2}-4\left(\frac{\boldsymbol{q}_1\cdot\boldsymbol{q}_{34}}{q_{34}^2}-\frac{1}{3}\right)\frac{\boldsymbol{k}\cdot\boldsymbol{q}_1}{q_1^2}\right]\right\}G_2(\boldsymbol{q}_3,\boldsymbol{q}_4)\\
&+\frac{5}{2}\left\{\left[\frac{2}{3}+\frac{\boldsymbol{q}_{12}\cdot\boldsymbol{q}_{34}}{q_{34}^2}\left(1-\frac{k^2}{q_{12}^2}\right)\right]\left(-\frac{2}{q_2^2}+\frac{\boldsymbol{q}_1\cdot\boldsymbol{q}_2}{q_1^2q_2^2}-\frac{3}{2}\frac{\boldsymbol{q}_{12}\cdot\boldsymbol{q}_1}{q_{12}^2q_1^2}-\frac{3}{2}\frac{\boldsymbol{q}_{12}\cdot\boldsymbol{q}_2}{q_{12}^2}\frac{\boldsymbol{q}_1\cdot\boldsymbol{q}_2}{q_1^2q_2^2}\right)\right.\\
&\qquad\left.+\frac{1}{q_2^2}\left[\frac{2}{3}\frac{\boldsymbol{q}_1\cdot\boldsymbol{q}_{34}}{q_1^2}-4\left(\frac{\boldsymbol{q}_1\cdot\boldsymbol{q}_{34}}{q_1^2}-\frac{1}{3}\right)\frac{\boldsymbol{k}\cdot\boldsymbol{q}_{34}}{q_{34}^2}\right]\right\}G_2(\boldsymbol{q}_3,\boldsymbol{q}_4)\\
&+\left\{\left[\frac{2}{3}+\frac{\boldsymbol{q}_1\cdot\boldsymbol{q}_{234}}{q_1^2}\left(1-\frac{k^2}{q_{234}^2}\right)\right]\left(-\frac{2}{q_{34}^2}+\frac{\boldsymbol{q}_2\cdot\boldsymbol{q}_{34}}{q_2^2q_{34}^2}-\frac{3}{2}\frac{\boldsymbol{q}_2\cdot\boldsymbol{q}_{234}}{q_2^2q_{234}^2}-\frac{3}{2}\frac{\boldsymbol{q}_{234}\cdot\boldsymbol{q}_{34}}{q_{234}^2}\frac{\boldsymbol{q}_2\cdot\boldsymbol{q}_{34}}{q_2^2q_{34}^2}\right)\right.\\
&\qquad\left.+\frac{1}{q_{34}^2}\left[\frac{2}{3}\frac{\boldsymbol{q}_1\cdot\boldsymbol{q}_2}{q_2^2}-4\left(\frac{\boldsymbol{q}_1\cdot\boldsymbol{q}_2}{q_2^2}-\frac{1}{3}\right)\frac{\boldsymbol{k}\cdot\boldsymbol{q}_1}{q_1^2}\right]\right\}\left[\frac{3}{2}F_2(\boldsymbol{q}_3,\boldsymbol{q}_4)+G_2(\boldsymbol{q}_3,\boldsymbol{q}_4)\right]\\
&+\left(-\frac{2}{3}-\frac{\boldsymbol{q}_1\cdot\boldsymbol{q}_{234}}{q_1^2}+\frac{k^2}{q_{234}^2}\frac{\boldsymbol{q}_1\cdot\boldsymbol{q}_{234}}{q_1^2}\right)\\
&\quad\times\frac{1}{4q_{34}^2}\left(-2+\frac{\boldsymbol{q}_2\cdot\boldsymbol{q}_{34}}{q_2^2}-\frac{3}{2}\frac{\boldsymbol{q}_{234}\cdot\boldsymbol{q}_2}{q_{234}^2}\frac{q_{34}^2}{q_2^2}-\frac{3}{2}\frac{\boldsymbol{q}_{234}\cdot\boldsymbol{q}_{34}}{q_{234}^2}\frac{\boldsymbol{q}_2\cdot\boldsymbol{q}_{34}}{q_{34}^2}\right)\left[1+\frac{\boldsymbol{q}_3\cdot\boldsymbol{q}_4}{q_3^2}\left(1-\frac{\boldsymbol{q}_{34}\cdot\boldsymbol{q}_4}{q_4^2}\right)\right]\\
&+\frac{1}{4q_{34}^2}\left(-\frac{2}{3}\frac{\boldsymbol{q}_1\cdot\boldsymbol{q}_2}{q_1^2}+4\frac{\boldsymbol{q}_1\cdot\boldsymbol{q}_2}{q_1^2}\frac{\boldsymbol{k}\cdot\boldsymbol{q}_2}{q_2^2}-\frac{4}{3}\frac{\boldsymbol{k}\cdot\boldsymbol{q}_2}{q_2^2}\right)\left[1+\frac{\boldsymbol{q}_3\cdot\boldsymbol{q}_4}{q_3^2}\left(1-\frac{\boldsymbol{q}_{34}\cdot\boldsymbol{q}_4}{q_4^2}\right)\right],
\end{aligned}
\tag{58}
$$

and

$$
\begin{aligned}
A_2 =& \frac{25}{4}\frac{\boldsymbol{q}_1\cdot\boldsymbol{q}_{234}}{q_{234}^2}\left(\frac{2}{q_4^2}-\frac{\boldsymbol{q}_{23}\cdot\boldsymbol{q}_4}{q_{23}^2q_4^2}+\frac{3}{2}\frac{\boldsymbol{q}_{234}\cdot\boldsymbol{q}_{23}}{q_{234}^2q_{23}^2}+\frac{3}{2}\frac{\boldsymbol{q}_{234}\cdot\boldsymbol{q}_4}{q_{234}^2}\frac{\boldsymbol{q}_{23}\cdot\boldsymbol{q}_4}{q_{23}^2q_4^2}\right)\left(\frac{2}{q_2^2}-\frac{\boldsymbol{q}_2\cdot\boldsymbol{q}_3}{q_2^2q_3^2}+\frac{3}{2}\frac{\boldsymbol{q}_{23}\cdot\boldsymbol{q}_2}{q_{23}^2q_2^2}+\frac{3}{2}\frac{\boldsymbol{q}_{23}\cdot\boldsymbol{q}_3}{q_{23}^2}\frac{\boldsymbol{q}_2\cdot\boldsymbol{q}_3}{q_2^2q_3^2}\right)\\
&-\frac{25}{8}\frac{\boldsymbol{q}_1\cdot\boldsymbol{q}_{234}}{q_{34}^2q_{234}^2}\left(-2+\frac{\boldsymbol{q}_2\cdot\boldsymbol{q}_{34}}{q_2^2}-\frac{3}{2}\frac{\boldsymbol{q}_{234}\cdot\boldsymbol{q}_2}{q_{234}^2}\frac{q_{34}^2}{q_2^2}-\frac{3}{2}\frac{\boldsymbol{q}_{234}\cdot\boldsymbol{q}_{34}}{q_{234}^2}\frac{\boldsymbol{q}_2\cdot\boldsymbol{q}_{34}}{q_{34}^2}\right)\frac{3\boldsymbol{q}_3\cdot\boldsymbol{q}_4+8q_4^2}{q_3^2q_4^2}\\
&+\frac{25}{4}\frac{\boldsymbol{q}_1\cdot\boldsymbol{q}_{234}}{q_{234}^2}\frac{1}{q_3^2q_4^2}\left[-4+4\frac{\boldsymbol{q}_2\cdot\boldsymbol{q}_3}{q_2^2}-\frac{3}{2}\left(\frac{\boldsymbol{q}_{234}\cdot\boldsymbol{q}_2}{q_{234}^2}\frac{\boldsymbol{q}_3\cdot\boldsymbol{q}_4}{q_2^2}+3\frac{\boldsymbol{q}_{234}\cdot\boldsymbol{q}_4}{q_{234}^2}\frac{\boldsymbol{q}_2\cdot\boldsymbol{q}_3}{q_2^2}+4\frac{\boldsymbol{q}_{234}\cdot\boldsymbol{q}_3}{q_{234}^2}\frac{\boldsymbol{q}_2\cdot\boldsymbol{q}_3}{q_2^2}+4\frac{\boldsymbol{q}_{234}\cdot\boldsymbol{q}_2}{q_{234}^2}\frac{q_3^2}{q_2^2}\right)\right]\\
&-\frac{25}{4}\frac{\boldsymbol{q}_1\cdot\boldsymbol{q}_2}{q_2^2q_{34}^2}\frac{3\boldsymbol{q}_3\cdot\boldsymbol{q}_4+8q_4^2}{q_3^2q_4^2}+\frac{25}{4}\frac{\boldsymbol{q}_1\cdot\boldsymbol{q}_{34}}{q_2^2q_{34}^2}\left[-\frac{2}{q_4^2}+\frac{\boldsymbol{q}_3\cdot\boldsymbol{q}_4}{q_3^2q_4^2}-\frac{3}{2}\frac{\boldsymbol{q}_{34}\cdot\boldsymbol{q}_3}{q_{34}^2q_3^2}-\frac{3}{2}\frac{\boldsymbol{q}_{34}\cdot\boldsymbol{q}_4}{q_{34}^2}\frac{\boldsymbol{q}_3\cdot\boldsymbol{q}_4}{q_3^2q_4^2}\right]-\frac{25}{q_3^2q_4^2}\frac{\boldsymbol{q}_1\cdot\boldsymbol{q}_2}{q_2^2}\,, \qquad (59)\\
B_2 =& \left(-\frac{2}{3}-\frac{\boldsymbol{q}_1\cdot\boldsymbol{q}_{234}}{q_1^2}+\frac{k^2}{q_{234}^2}\frac{\boldsymbol{q}_1\cdot\boldsymbol{q}_{234}}{q_1^2}\right)\\
&\times\left\{\frac{25}{4}\left(\frac{2}{q_4^2}-\frac{\boldsymbol{q}_{23}\cdot\boldsymbol{q}_4}{q_{23}^2q_4^2}+\frac{3}{2}\frac{\boldsymbol{q}_{234}\cdot\boldsymbol{q}_{23}}{q_{234}^2q_{23}^2}+\frac{3}{2}\frac{\boldsymbol{q}_{234}\cdot\boldsymbol{q}_4}{q_{234}^2}\frac{\boldsymbol{q}_{23}\cdot\boldsymbol{q}_4}{q_{23}^2q_4^2}\right)\left(\frac{2}{q_3^2}-\frac{\boldsymbol{q}_2\cdot\boldsymbol{q}_3}{q_2^2q_3^2}+\frac{3}{2}\frac{\boldsymbol{q}_{23}\cdot\boldsymbol{q}_2}{q_{23}^2q_2^2}+\frac{3}{2}\frac{\boldsymbol{q}_{23}\cdot\boldsymbol{q}_3}{q_{23}^2}\frac{\boldsymbol{q}_2\cdot\boldsymbol{q}_3}{q_2^2q_3^2}\right)\right.\\
&\quad-\frac{25}{8q_{34}^2}\left(-2+\frac{\boldsymbol{q}_2\cdot\boldsymbol{q}_{34}}{q_2^2}-\frac{3}{2}\frac{\boldsymbol{q}_{234}\cdot\boldsymbol{q}_2}{q_{234}^2}\frac{q_{34}^2}{q_2^2}-\frac{3}{2}\frac{\boldsymbol{q}_{234}\cdot\boldsymbol{q}_{34}}{q_{234}^2}\frac{\boldsymbol{q}_2\cdot\boldsymbol{q}_{34}}{q_{34}^2}\right)\frac{3\boldsymbol{q}_3\cdot\boldsymbol{q}_4+8q_4^2}{q_3^2q_4^2}\\
&\left.\quad+\frac{25}{4q_3^2q_4^2}\left[-4+4\frac{\boldsymbol{q}_2\cdot\boldsymbol{q}_3}{q_2^2}-\frac{3}{2}\left(\frac{\boldsymbol{q}_{234}\cdot\boldsymbol{q}_2}{q_{234}^2}\frac{\boldsymbol{q}_3\cdot\boldsymbol{q}_4}{q_2^2}+3\frac{\boldsymbol{q}_{234}\cdot\boldsymbol{q}_4}{q_{234}^2}\frac{\boldsymbol{q}_2\cdot\boldsymbol{q}_3}{q_2^2}+4\frac{\boldsymbol{q}_{234}\cdot\boldsymbol{q}_3}{q_{234}^2}\frac{\boldsymbol{q}_2\cdot\boldsymbol{q}_3}{q_2^2}+4\frac{\boldsymbol{q}_{234}\cdot\boldsymbol{q}_2}{q_{234}^2}\frac{q_3^2}{q_2^2}\right)\right]\right\}\\
&-\frac{25}{8q_{34}^2}\left(-\frac{2}{3}\frac{\boldsymbol{q}_1\cdot\boldsymbol{q}_2}{q_1^2}+4\frac{\boldsymbol{q}_1\cdot\boldsymbol{q}_2}{q_1^2}\frac{\boldsymbol{k}\cdot\boldsymbol{q}_2}{q_2^2}-\frac{4}{3}\frac{\boldsymbol{k}\cdot\boldsymbol{q}_2}{q_2^2}\right)\frac{3\boldsymbol{q}_3\cdot\boldsymbol{q}_4+8q_4^2}{q_3^2q_4^2}\\
&+\frac{25}{4q_1^2}\left(-\frac{2}{q_4^2}+\frac{\boldsymbol{q}_3\cdot\boldsymbol{q}_4}{q_3^2q_4^2}-\frac{3}{2}\frac{\boldsymbol{q}_{34}\cdot\boldsymbol{q}_3}{q_{34}^2q_3^2}-\frac{3}{2}\frac{\boldsymbol{q}_{34}\cdot\boldsymbol{q}_4}{q_{34}^2}\frac{\boldsymbol{q}_3\cdot\boldsymbol{q}_4}{q_3^2q_4^2}\right)\\
&\quad\times\left(4\frac{\boldsymbol{k}\cdot\boldsymbol{q}_2}{q_2^2}\frac{\boldsymbol{q}_2\cdot\boldsymbol{q}_{34}}{q_{34}^2}-\frac{4}{3}\frac{\boldsymbol{k}\cdot\boldsymbol{q}_2}{q_2^2}+4\frac{\boldsymbol{k}\cdot\boldsymbol{q}_{34}}{q_{34}^2}\frac{\boldsymbol{q}_2\cdot\boldsymbol{q}_{34}}{q_2^2}-\frac{4}{3}\frac{\boldsymbol{k}\cdot\boldsymbol{q}_{34}}{q_{34}^2}-\frac{2}{3}\frac{\boldsymbol{q}_2\cdot\boldsymbol{q}_{34}}{q_{34}^2}-\frac{8}{3}\frac{\boldsymbol{q}_2\cdot\boldsymbol{q}_{34}}{{q_2}^2}\right)\\
&+\frac{25}{4q_1^2q_2^2}\left(12\frac{\boldsymbol{q}_3\cdot\boldsymbol{q}_4}{q_3^2}\frac{\boldsymbol{k}\cdot\boldsymbol{q}_4}{q_4^2}-4\frac{\boldsymbol{k}\cdot\boldsymbol{q}_4}{q_4^2}-4\frac{\boldsymbol{q}_3\cdot\boldsymbol{q}_4}{q_3^2}+2\frac{\boldsymbol{q}_1\cdot\boldsymbol{q}_2}{q_3^2}\frac{\boldsymbol{q}_3\cdot\boldsymbol{q}_4}{q_4^2}+\frac{2}{3}\frac{\boldsymbol{q}_1\cdot\boldsymbol{q}_3}{q_3^2}\frac{\boldsymbol{q}_2\cdot\boldsymbol{q}_4}{q_4^2}\right)\\
&+\frac{25}{4}\left(\frac{2}{3}-\frac{\boldsymbol{k}\cdot\boldsymbol{q}_{34}}{q_{34}^2}+\frac{\boldsymbol{k}\cdot\boldsymbol{q}_{34}}{q_{34}^2}\frac{\boldsymbol{q}_{12}\cdot\boldsymbol{q}_{34}}{q_{12}^2}\right)\\
&\quad\times\left(\frac{2}{q_2^2}-\frac{\boldsymbol{q}_1\cdot\boldsymbol{q}_2}{q_1^2q_2^2}+\frac{3}{2}\frac{\boldsymbol{q}_{12}\cdot\boldsymbol{q}_1}{q_{12}^2q_1^2}+\frac{3}{2}\frac{\boldsymbol{q}_{12}\cdot\boldsymbol{q}_2}{q_{12}^2}\frac{\boldsymbol{q}_1\cdot\boldsymbol{q}_2}{q_1^2q_2^2}\right)\left(\frac{2}{q_4^2}-\frac{\boldsymbol{q}_3\cdot\boldsymbol{q}_4}{q_3^2q_4^2}+\frac{3}{2}\frac{\boldsymbol{q}_{34}\cdot\boldsymbol{q}_3}{q_{34}^2q_3^2}+\frac{3}{2}\frac{\boldsymbol{q}_{34}\cdot\boldsymbol{q}_4}{q_{34}^2}\frac{\boldsymbol{q}_3\cdot\boldsymbol{q}_4}{q_3^2q_4^2}\right). \qquad (60)
\end{aligned}
$$

The fully symmetric kernels can be obtained by taking into account possible permutations,

$$F_4^{(s)}(\boldsymbol{q}_1,\boldsymbol{q}_2,\boldsymbol{q}_3,\boldsymbol{q}_4) = \frac{1}{4!}\Big[F_4(\boldsymbol{q}_1,\boldsymbol{q}_2,\boldsymbol{q}_3,\boldsymbol{q}_4)+(23\text{ cyclic})\Big]\,, \qquad (61)$$

$$G_4^{(s)}(\boldsymbol{q}_1,\boldsymbol{q}_2,\boldsymbol{q}_3,\boldsymbol{q}_4) = \frac{1}{4!}\Big[G_4(\boldsymbol{q}_1,\boldsymbol{q}_2,\boldsymbol{q}_3,\boldsymbol{q}_4)+(23\text{ cyclic})\Big]\,. \qquad (62)$$

Note that the equations and solutions up to third order can be found in [15].

References

[1] C. L. Bennett *et al.* [WMAP Collaboration], Astrophys. J. Suppl. **208**, 20 (2013) [arXiv:1212.5225 [astro-ph.CO]] ; G. Hinshaw *et al.* [WMAP Collaboration], Astrophys. J. Suppl. **208**, 19 (2013) [arXiv:1212.5226 [astro-ph.CO]].

[2] P. A. R. Ade *et al.* [Planck Collaboration], arXiv:1303.5062 [astro-ph.CO] ; P. A. R. Ade *et al.* [Planck Collaboration], arXiv:1303.5076 [astro-ph.CO].

[3] A. Kogut, D. J. Fixsen, D. T. Chuss, J. Dotson, E. Dwek, M. Halpern, G. F. Hinshaw and S. M. Meyer *et al.*, JCAP **1107**, 025 (2011) [arXiv:1105.2044 [astro-ph.CO]].

[4] P. Andr *et al.* [PRISM Collaboration], arXiv:1310.1554 [astro-ph.CO].

[5] T. Matsumura, Y. Akiba, J. Borrill, Y. Chinone, M. Dobbs, H. Fuke, A. Ghribi and M. Hasegawa *et al.*, arXiv:1311.2847 [astro-ph.IM].

[6] L. Anderson *et al.* [BOSS Collaboration], arXiv:1312.4877 [astro-ph.CO].

[7] C. Blake, E. Kazin, F. Beutler, T. Davis, D. Parkinson, S. Brough, M. Colless and C. Contreras *et al.*, Mon. Not. Roy. Astron. Soc. **418**, 1707 (2011) [arXiv:1108.2635 [astro-ph.CO]].

[8] S. de la Torre, L. Guzzo, J. A. Peacock, E. Branchini, A. Iovino, B. R. Granett, U. Abbas and C. Adami *et al.*, arXiv:1303.2622 [astro-ph.CO].

[9] http://desi.lbl.gov

[10] http://www.hetdex.org

[11] http://www.lsst.org/lsst/

[12] http://sci.esa.int/euclid/

[13] For a recent collection of reviews, see e.g. Class. Quant. Grav. **27**, "Focus section on non-linear and non-Gaussian cosmological perturbations" (2010) ; Adv. Astron. **2010**, "Testing the Gaussianity and Statistical Isotropy of the Universe" (2010).

[14] B. Jain and E. Bertschinger, Astrophys. J. **431**, 495 (1994) [astro-ph/9311070] ; D. Jeong and E. Komatsu, Astrophys. J. **651**, 619 (2006) [arXiv:astro-ph/0604075].

[15] D. Jeong, J. O. Gong, H. Noh and J. c. Hwang, Astrophys. J. **727**, 22 (2011) [arXiv:1010.3489 [astro-ph.CO]].

[16] F. Bernardeau, S. Colombi, E. Gaztanaga and R. Scoccimarro, Phys. Rept. **367**, 1 (2002) [arXiv:astro-ph/0112551].

[17] D. H. Weinberg, M. J. Mortonson, D. J. Eisenstein, C. Hirata, A. G. Riess and E. Rozo, Phys. Rept. **530**, 87 (2013) [arXiv:1201.2434 [astro-ph.CO]].

[18] J. -c. Hwang, H. Noh and J. -O. Gong, Astrophys. J. **752**, 50 (2012) [arXiv:1204.3345 [astro-ph.CO]].

[19] J. Yoo, A. L. Fitzpatrick and M. Zaldarriaga, Phys. Rev. D **80**, 083514 (2009) [arXiv:0907.0707 [astro-ph.CO]] ; C. Bonvin and R. Durrer, Phys. Rev. D **84**, 063505 (2011) [arXiv:1105.5280 [astro-ph.CO]] ; A. Challinor and A. Lewis, Phys. Rev. D **84**, 043516 (2011) [arXiv:1105.5292 [astro-ph.CO]] ; D. Jeong, F. Schmidt and C. M. Hirata, Phys. Rev. D **85**, 023504 (2012) [arXiv:1107.5427 [astro-ph.CO]].

[20] H. Noh and J. c. Hwang, Phys. Rev. D **69**, 104011 (2004) [arXiv:astro-ph/0305123].

[21] R. L. Arnowitt, S. Deser and C. W. Misner, arXiv:gr-qc/0405109.

[22] J. M. Bardeen, Phys. Rev. D **22**, 1882 (1980).

[23] R. Scoccimarro, Astrophys. J. **487**, 1 (1997) [astro-ph/9612207].

[24] E. Komatsu *et al.* [WMAP Collaboration], Astrophys. J. Suppl. **192**, 18 (2011) [arXiv:1001.4538 [astro-ph.CO]].